

**Supplemental Figures, Legends, Methods, Tables, and References for:**

**EGFR Regulates Macrophage Activation and Function in Bacterial Infection**

Dana M. Harbower<sup>1,2</sup>, Kshipra Singh<sup>2</sup>, Mohammad Asim<sup>2</sup>, Thomas G. Verriere<sup>2</sup>, Danyvid Olivares-Villagómez<sup>1</sup>, Daniel P. Barry<sup>2</sup>, Margaret M. Allaman<sup>2</sup>, M. Kay Washington<sup>1</sup>, Richard M. Peek, Jr.<sup>2,3</sup>,  
M. Blanca Piazuelo<sup>2</sup>, and Keith T. Wilson<sup>1,2,3,4,5</sup>

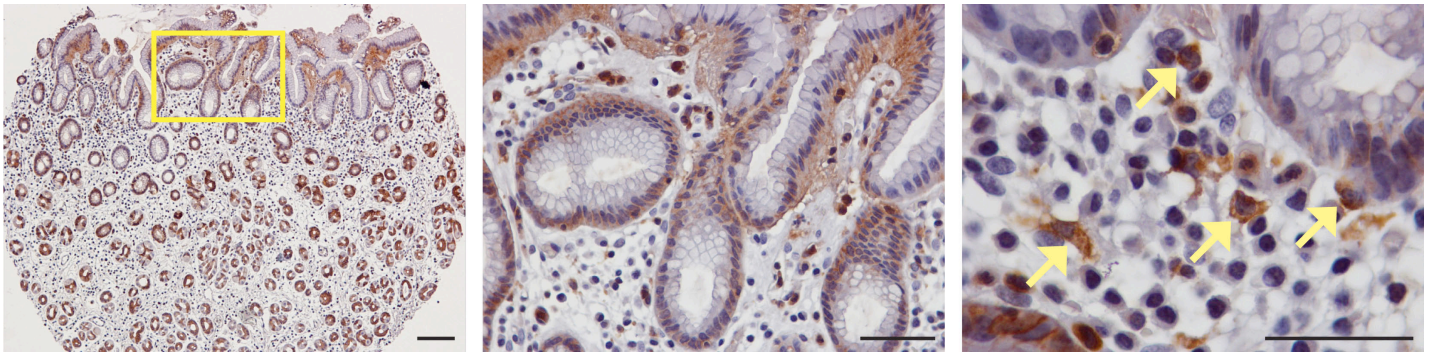
<sup>1</sup>Department of Pathology, Microbiology, and Immunology; Vanderbilt University Medical Center; Nashville, TN, USA

<sup>2</sup>Division of Gastroenterology, Hepatology, and Nutrition, Department of Medicine; Vanderbilt University Medical Center; Nashville, TN, USA

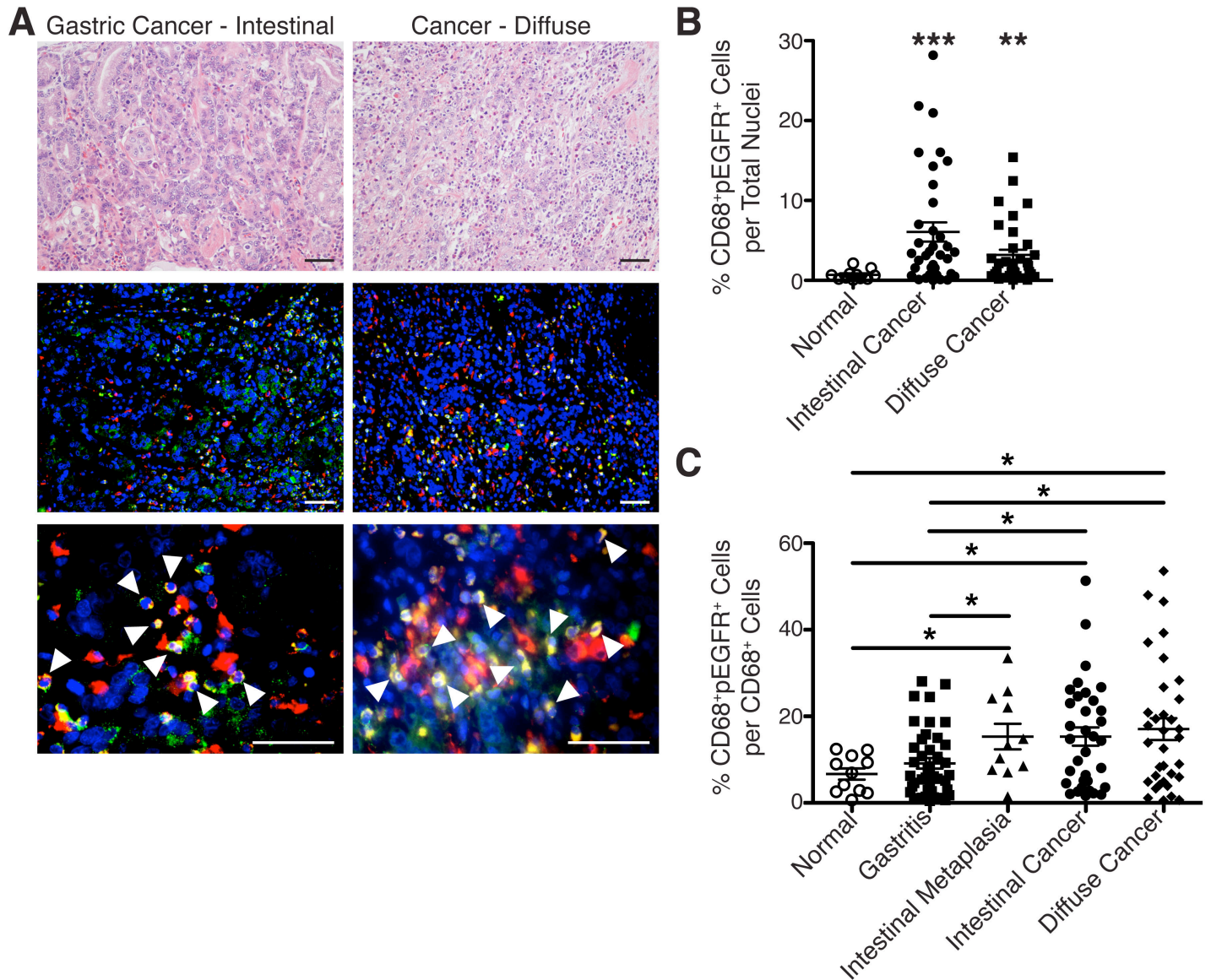
<sup>3</sup>Department of Cancer Biology; Vanderbilt University Medical Center; Nashville, TN, USA

<sup>4</sup>Center for Mucosal Inflammation and Cancer, Vanderbilt University Medical Center; Nashville, TN, USA

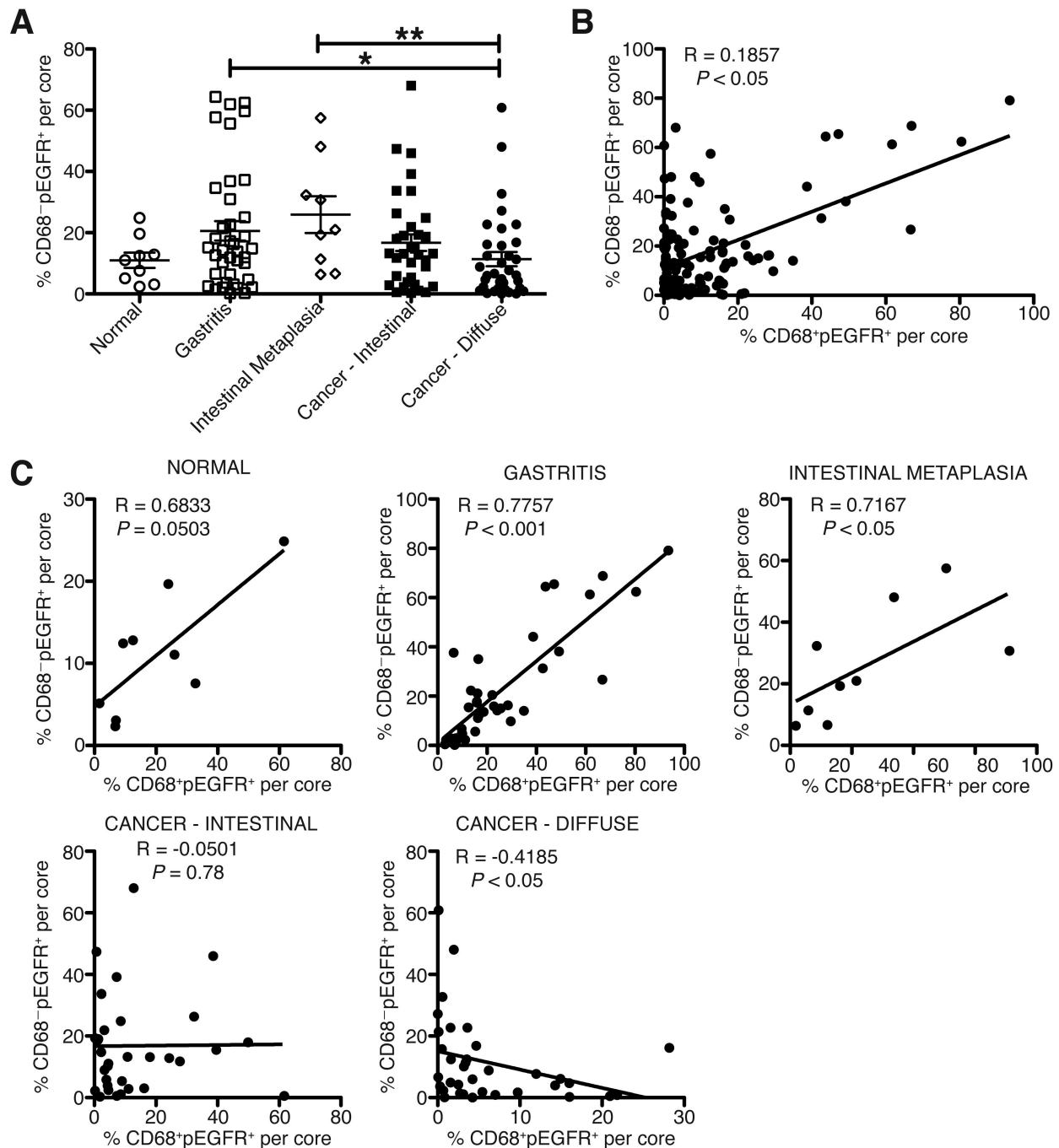
<sup>5</sup>Veterans Affairs Tennessee Valley Healthcare System; Nashville, TN, USA



**Supplemental Figure 1. Mononuclear cells in human gastritis tissues have high levels of pEGFR.** Representative image of a gastric tissue core from the Vanderbilt University Medical Center human tissue microarray (TMA) assessed for pEGFR expression by immunoperoxidase staining. Middle and right images are magnifications of the area in the yellow box in the left image. Yellow arrows indicate pEGFR<sup>+</sup> mononuclear cells. Scale bars = 100  $\mu$ M.  $n = 41$  gastritis samples.



**Supplemental Figure 2. CD68<sup>+</sup>pEGFR<sup>+</sup> macrophages are present in human cases of gastric cancer.** (A) Representative hematoxylin and eosin (H&E) and immunofluorescence images for cases of intestinal type and diffuse type gastric adenocarcinoma from the Vanderbilt University Medical Center human TMA. Red = CD68, Green = EGFR pY1068, Yellow = merge and Blue = DAPI. Scale bars = 50  $\mu$ M. White arrows indicate CD68<sup>+</sup>pEGFR<sup>+</sup> macrophages.  $n = 12$  normal samples, 35 intestinal-type cancer, and 35 diffuse-type cancer. (B) Quantification of the percentage of CD68<sup>+</sup>pEGFR<sup>+</sup> macrophages per the total number of cells in each individual core.  $**P < 0.01$ ,  $***P < 0.001$  vs. Normal.  $n = 12$  normal samples, 35 intestinal-type cancer, and 35 diffuse-type cancer. (C) Quantification of the percentage of CD68<sup>+</sup>pEGFR<sup>+</sup> macrophages per the total number of CD68<sup>+</sup> cells in each individual core.  $*P < 0.05$ .  $n = 12$  normal samples, 41 gastritis samples, 11 intestinal metaplasia samples, 35 intestinal-type cancer, and 35 diffuse-type cancer. In (B) and (C), statistical significance was calculated by one-way ANOVA with Kruskal-Wallis test, followed by Mann-Whitney  $U$  test. Note: The “Normal” data displayed in Panels B and C is the same “Normal” data as in Figure 1D, since there was only one set of normal biopsies on the TMA.



**Supplemental Figure 3. pEGFR levels in CD68<sup>+</sup> macrophages and CD68<sup>-</sup> cells are correlated in pre-cancerous stages, but not during cancer.** (A) Quantification of the percentage of CD68<sup>-</sup>pEGFR<sup>+</sup> cells per the total number of cells in each individual core from the TMA utilized in Figure 1 and in Supplemental Figures 1 and 2. \* $P < 0.05$ , \*\* $P < 0.01$ . Statistical significance was calculated by one-way ANOVA with Kruskal-Wallis test, followed by Mann-Whitney  $U$  test. (B) Overall correlation between CD68<sup>+</sup>pEGFR<sup>+</sup> macrophages and CD68<sup>-</sup>pEGFR<sup>+</sup> cells; data are from all cores in the TMA. (C) Correlation between CD68<sup>+</sup>pEGFR<sup>+</sup> macrophages and CD68<sup>-</sup>pEGFR<sup>+</sup> cells in each core in cases within the same histologic stage of disease. Correlation in (B) and (C) was calculated using the Spearman's rank correlation coefficient. In all panels,  $n = 12$  normal samples, 41 gastritis samples, 9 intestinal metaplasia samples, 35 intestinal-type cancer, and 35 diffuse-type cancer.

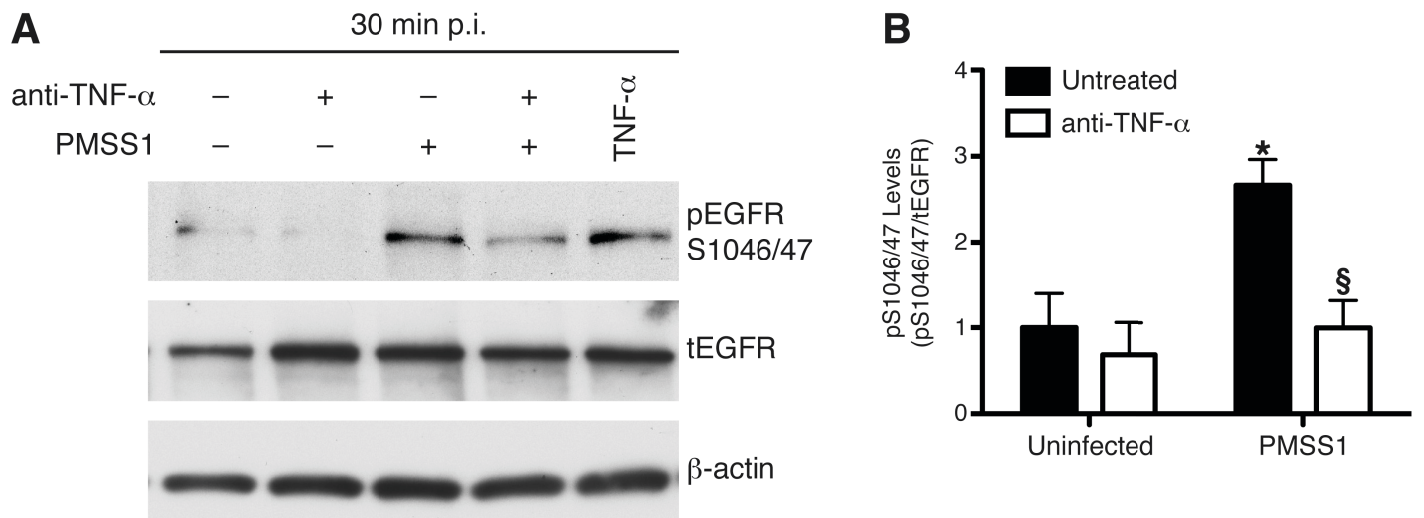
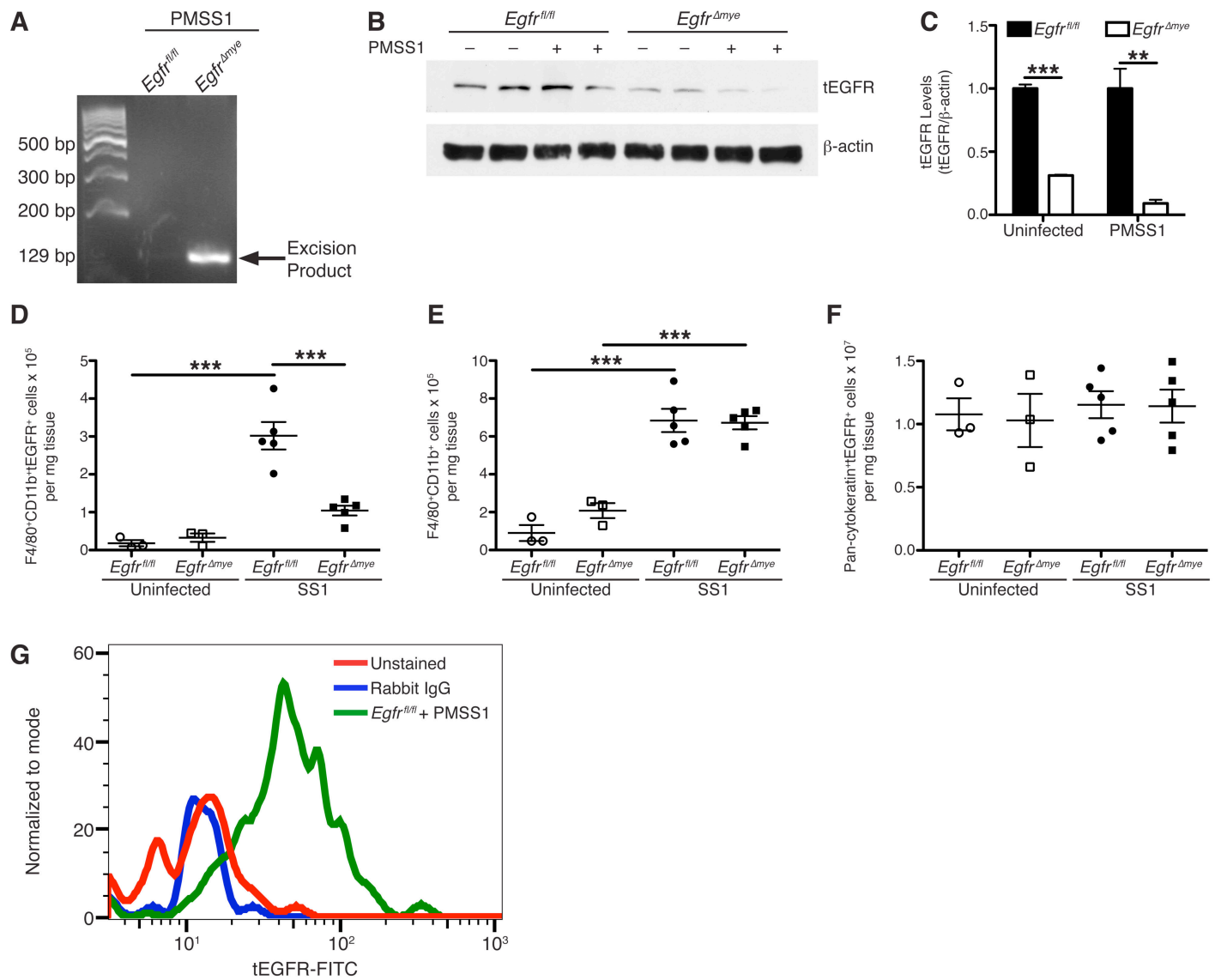
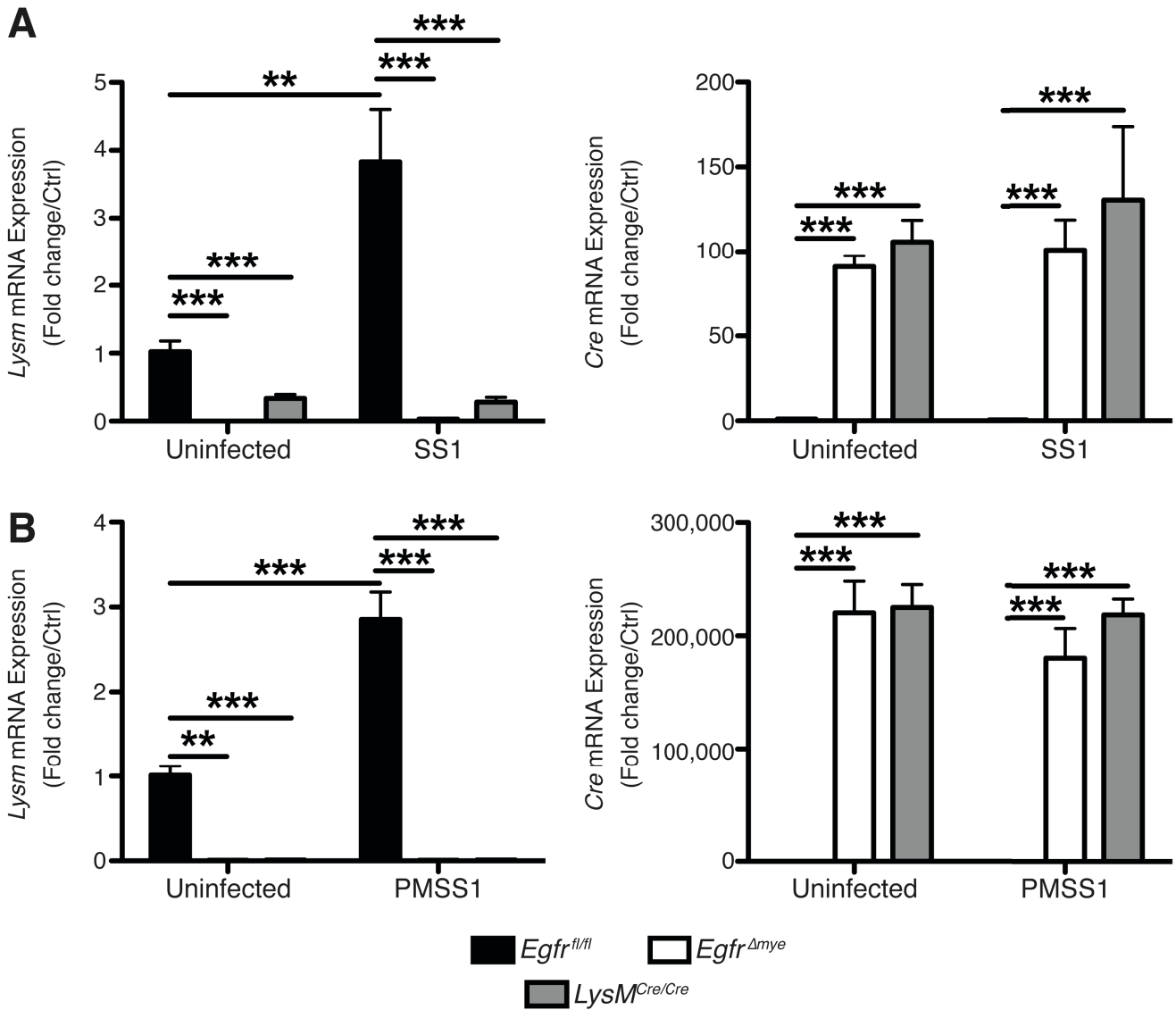


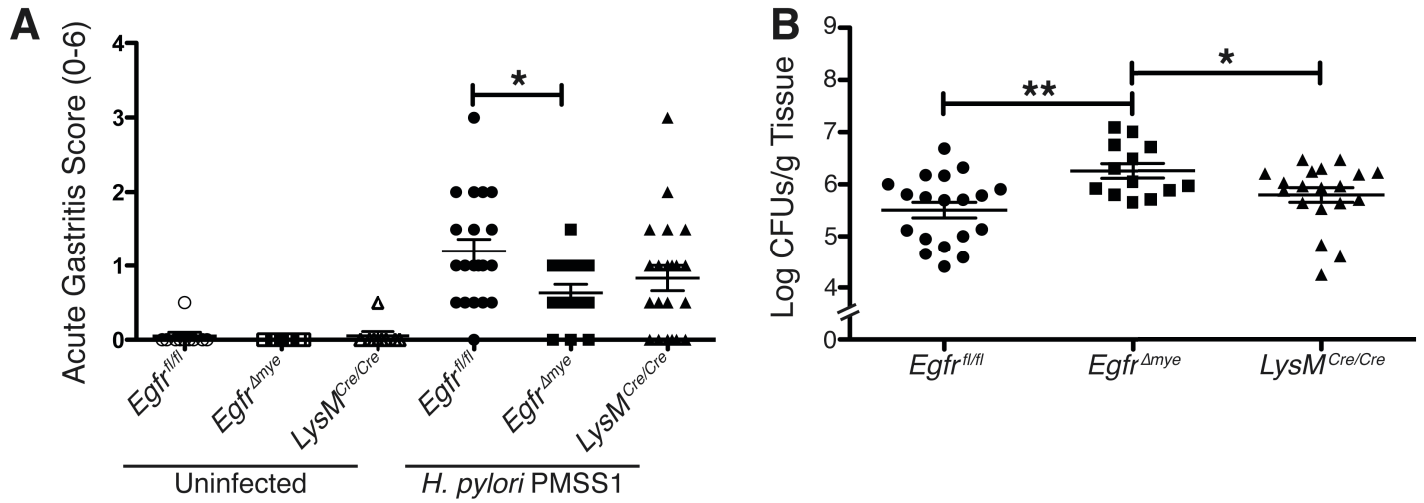
**Figure 4. EGFR phosphorylation in macrophages is ligand-independent and TNF- $\alpha$  dependent at the pS1046/47 residue.** (A) Representative western blot of pEGFR S1046/47 in RAW 264.7 cells at 30 min p.i.  $\pm$  anti-TNF- $\alpha$  neutralizing antibody (10 ng/mL) with *H. pylori* PMSS1 infection. Recombinant murine TNF- $\alpha$  (20 ng/mL) also stimulates pS1046/47 at 30 min post-stimulation.  $n = 3$  biological replicates. (B) Densitometric analysis of the levels of pS1046/47 in (A). \* $P < 0.05$  vs. uninfected, untreated control. § $P < 0.05$  vs. untreated, PMSS1-infected cells.  $n = 3$  biological replicates. Statistical significance was calculated by one-way ANOVA with Newman-Keuls post-test.



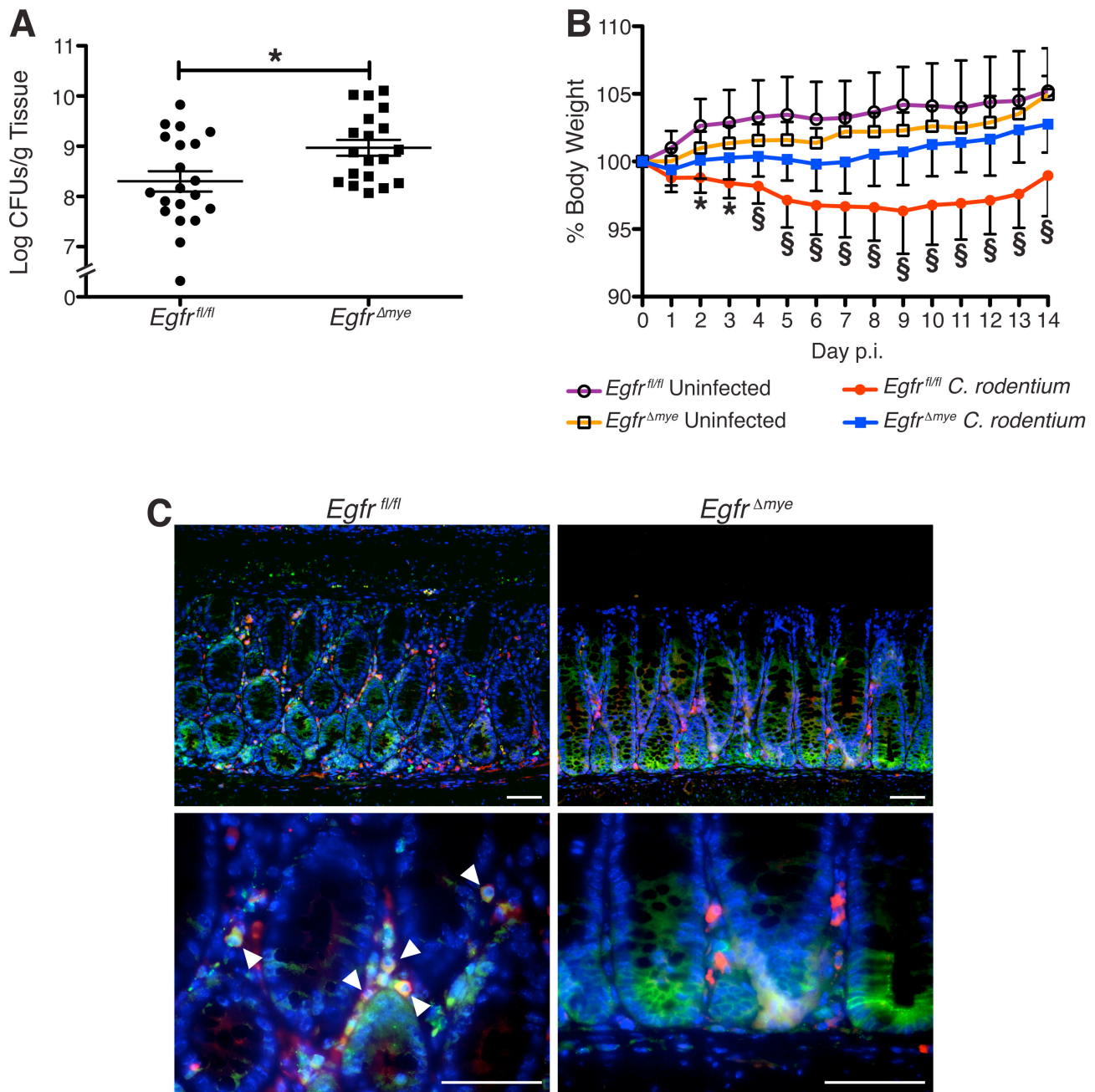
**Supplemental Figure 5. Confirmation of EGFR deletion in *Egfr<sup>Δmye</sup>* bone marrow-derived macrophages and gastric macrophages before and after infection with *H. pylori*.** (A) Representative DNA gel of PCR confirmation of *Egfr* excision in *Egfr<sup>Δmye</sup>* bone marrow-derived macrophages (BMmacs) 24 h post-infection (p.i.) with *H. pylori* PMSS1.  $n = 3$  biological replicates. (B) Representative western blot confirming tEGFR knockdown in *Egfr<sup>Δmye</sup>* BMmacs 24 h p.i. with *H. pylori* PMSS1. (C) Densitometric analysis of tEGFR levels from (B).  $**P < 0.01$ ,  $***P < 0.001$ . Statistical significance was calculated by Student's  $t$  test between uninfected *Egfr<sup>fl/fl</sup>* and *Egfr<sup>Δmye</sup>* BMmacs and between infected *Egfr<sup>fl/fl</sup>* and *Egfr<sup>Δmye</sup>* BMmacs. (D) Confirmation of tEGFR knockdown in F4/80<sup>+</sup>CD11b<sup>+</sup> gastric macrophages (Gmacs) from *Egfr<sup>Δmye</sup>* mice 48 h p.i. with *H. pylori* SS1 by flow cytometry.  $***P < 0.001$ .  $n = 3$  uninfected and 5 *H. pylori* SS1 infected mice per genotype. (E) Assessment of the total number of F4/80<sup>+</sup>CD11b<sup>+</sup> Gmacs in the stomachs of *Egfr<sup>fl/fl</sup>* and *Egfr<sup>Δmye</sup>* mice from (D) by flow cytometry.  $***P < 0.001$ .  $n = 3$  uninfected and 5 *H. pylori* SS1 infected mice per genotype. Statistical significance in (D) and (E) was calculated by one-way ANOVA with Newman-Keuls post-test. (F) Assessment of tEGFR levels in pan-cytokeratin<sup>+</sup> gastric epithelial cells from the same *Egfr<sup>fl/fl</sup>* and *Egfr<sup>Δmye</sup>* mice in (D) and (E).  $n = 3$  uninfected and 5 *H. pylori* SS1 infected mice per genotype. (G) Representative flow cytometry tracings of tEGFR staining, including a rabbit IgG isotype control from (D). The population of interest was first selected by gating on the F4/80<sup>+</sup>CD11b<sup>+</sup> cells and then assessing tEGFR-FITC staining.



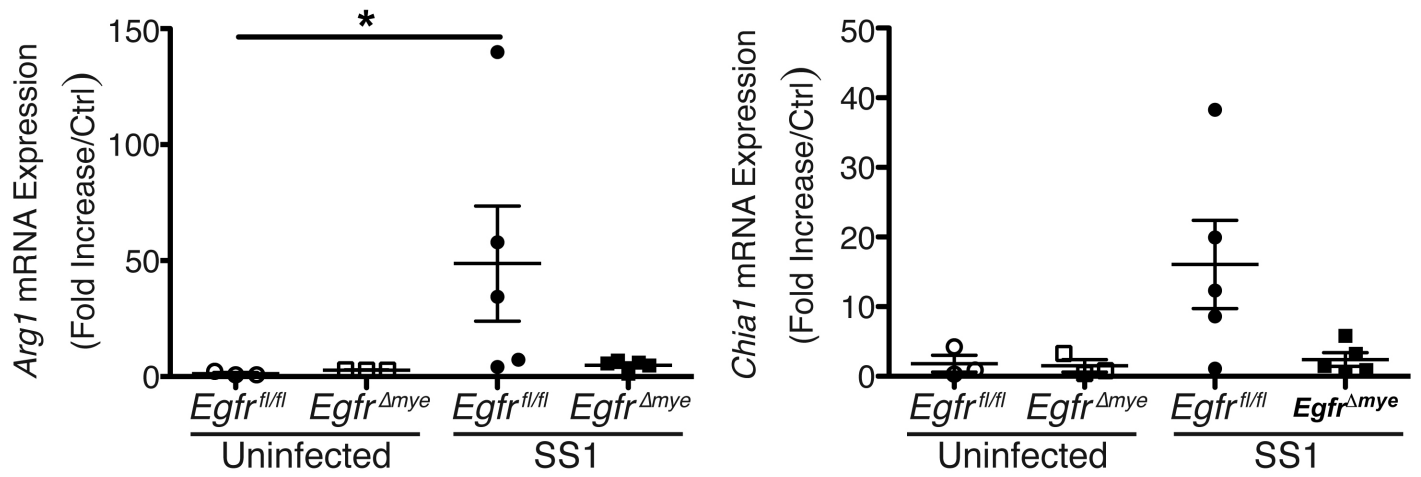
**Supplemental Figure 6. *Egfr<sup>Δmye</sup>* gastric tissues and BMmacs have no *Lysm* expression and substantial *Cre* expression.** (A) *Lysm* (*Lyz2*) and *Cre* mRNA levels were assessed by RT-PCR in *Egfr<sup>fl/fl</sup>*, *Egfr<sup>Δmye</sup>*, and *LysM<sup>Cre/Cre</sup>* gastric tissues 4 mo p.i. with *H. pylori* SS1. \*\* $P < 0.01$ , \*\*\* $P < 0.001$ .  $n = 3$  uninfected and 8 infected mice per genotype. (B) *Lysm* and *Cre* mRNA levels were assessed by RT-PCR in *Egfr<sup>fl/fl</sup>*, *Egfr<sup>Δmye</sup>*, and *LysM<sup>Cre/Cre</sup>* BMmacs 24 h p.i. with *H. pylori* PMSS1. \*\* $P < 0.01$ , \*\*\* $P < 0.001$ .  $n = 3$  biological replicates per genotype. Statistical significance in all panels was calculated by one-way ANOVA with Newman-Keuls post-test.



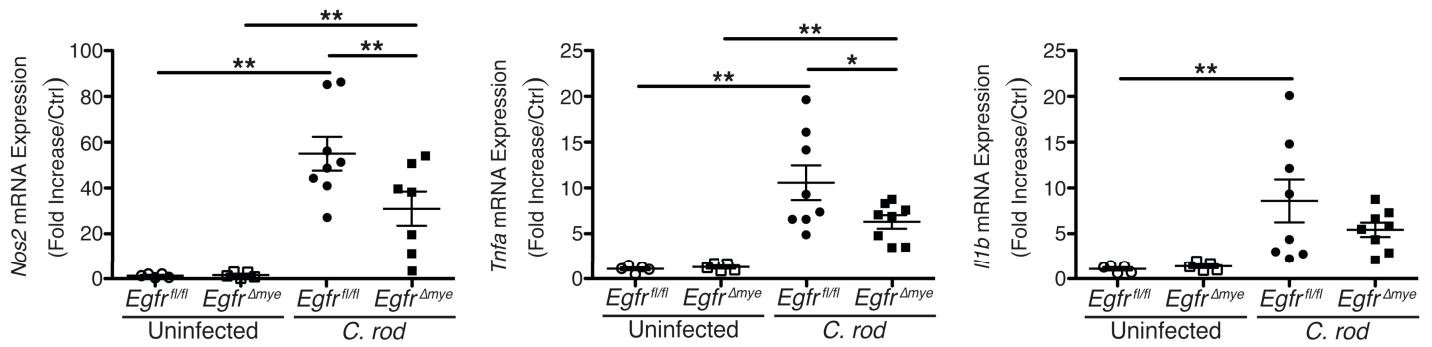
**Supplemental Figure 7. *Egfr<sup>Δmye</sup>* mice have increased bacterial burden and decreased disease pathology during acute *H. pylori* infection.** (A) Acute gastritis, specifically scoring neutrophilic infiltrate, was assessed 1 mo p.i by a gastrointestinal pathologist, according to the updated Sydney System, in a blinded manner. \* $P < 0.05$ .  $n = 8-10$  uninfected and 15-21 *H. pylori* PMSS1 infected mice per genotype. (B) Colonization levels of *H. pylori* PMSS1 were assessed 1 mo p.i. by serial dilution and culture. \* $P < 0.05$ , \*\* $P < 0.01$ .  $n = 15-21$  *H. pylori* PMSS1 infected mice per genotype. Significance in all panels was calculated by one-way ANOVA with Newman-Keuls post-test.



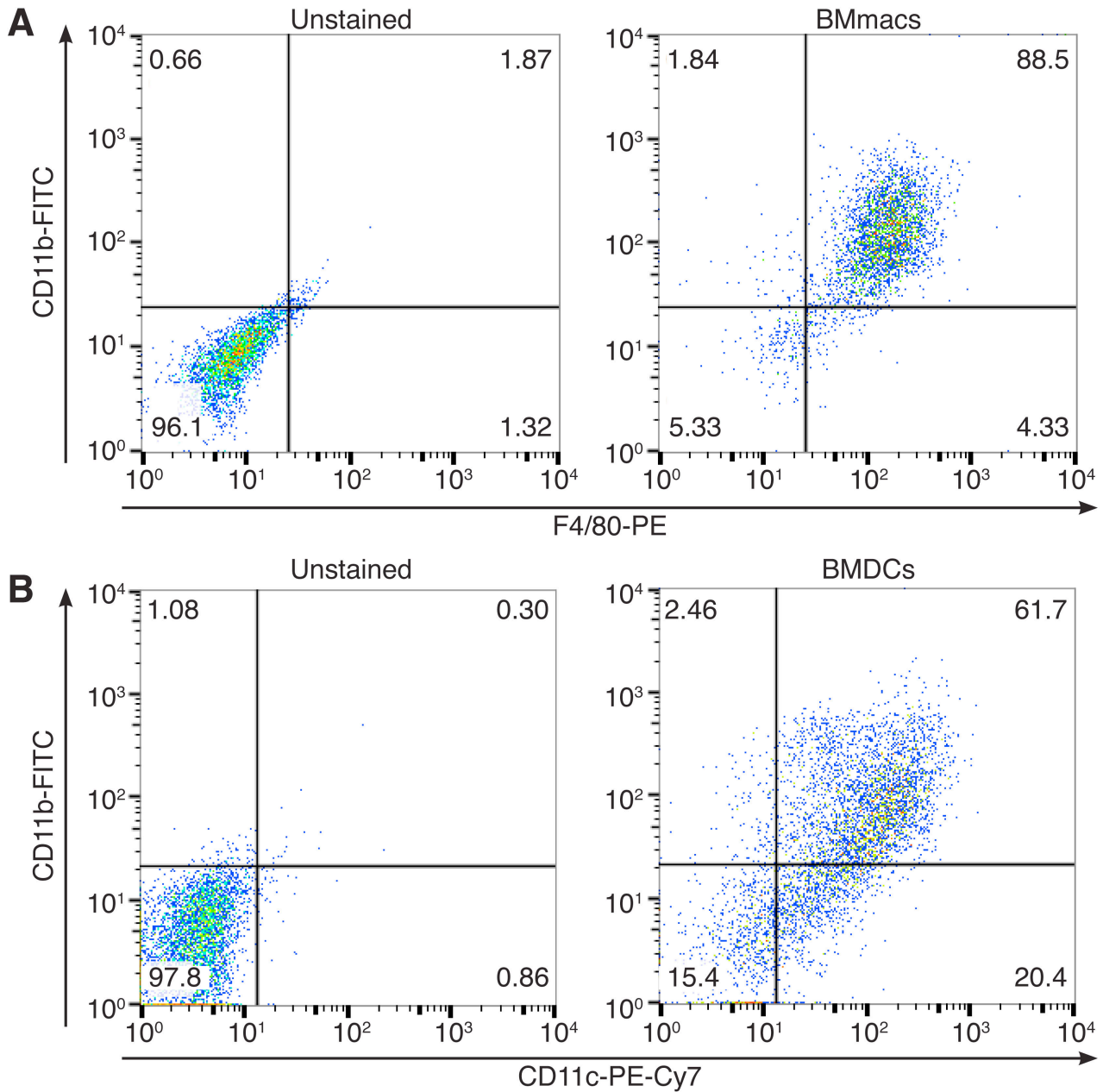
**Supplemental Figure 8. *Egfr<sup>Δmye</sup>* mice have increased bacterial burden and decreased clinical disease severity during *C. rodentium* infection.** (A) Colonization levels of *C. rodentium* in colonic tissues were assessed 14 d p.i. by serial dilution and culture. \* $P < 0.05$ .  $n = 8-10$  uninfected and 19-20 *C. rodentium* infected mice per genotype. Statistical significance was calculated by Student's  $t$  test (B) Percentage of initial body weight was assessed on each day of the 14-day infection model. \* $P < 0.01$ , § $P < 0.001$  vs. *Egfr<sup>fl/fl</sup>* *C. rodentium*.  $n = 8-10$  uninfected and 19-20 *C. rodentium* infected mice per genotype. Statistical significance was calculated by one-way ANOVA with the Kruskal-Wallis test, followed by Mann-Whitney  $U$  test. (C) Representative immunofluorescence images of pEGFR from infected mice in (A) and (B). Green = EGFR pY1068, Red = CD68, Yellow = merge, Blue = DAPI. Arrows indicate CD68<sup>+</sup>pEGFR<sup>+</sup> macrophages. Scale bars = 50  $\mu$ M.  $n \geq 3$  mice per genotype.



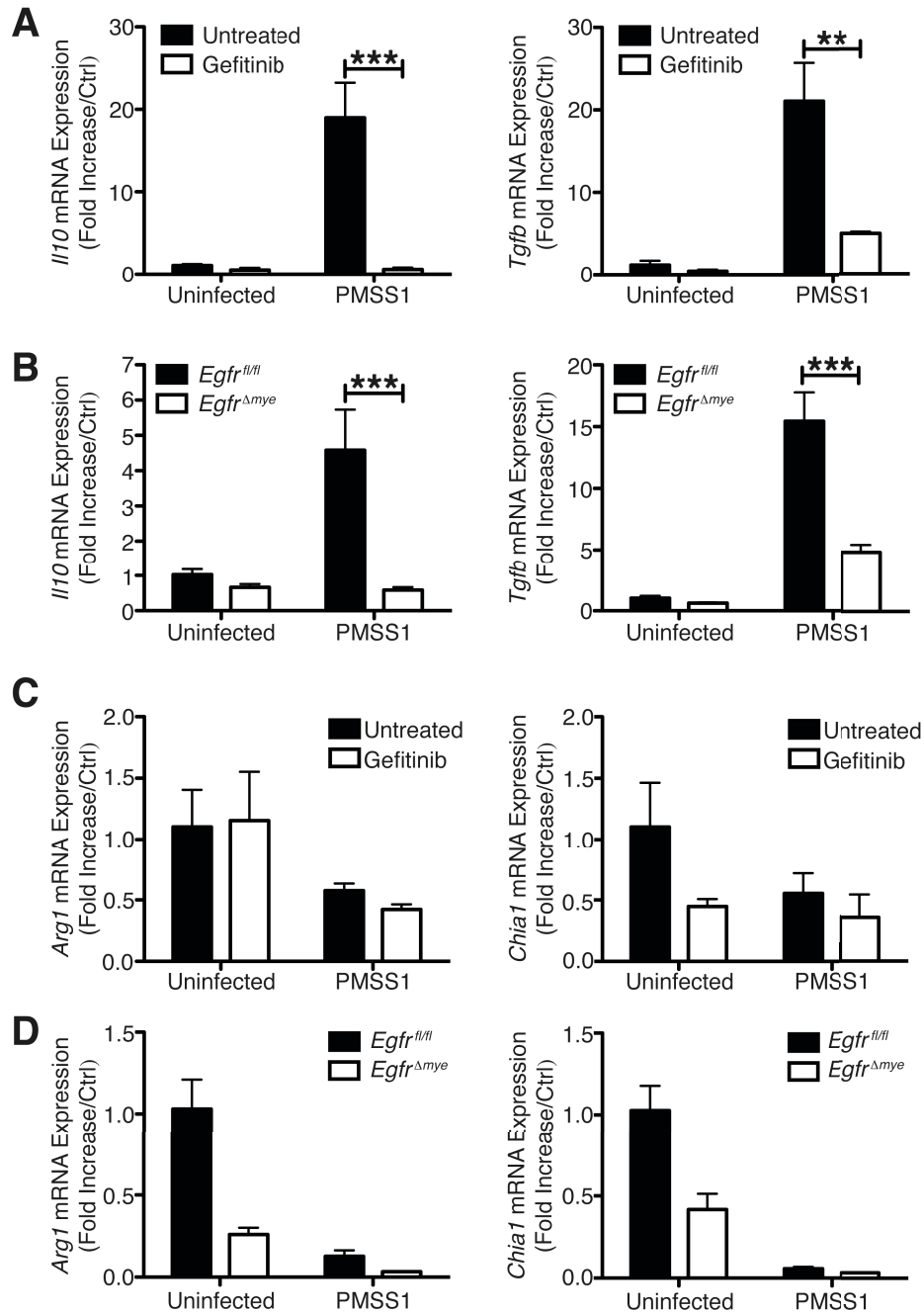
**Supplemental Figure 9. Markers of M2 activation are not significantly altered in *Egfr*<sup>Δmye</sup> gastric tissue during infection with *H. pylori*.** *Arg1* and *Chia1* mRNA expression was assessed by RT-PCR in gastric tissues 4 mo p.i. with *H. pylori* SS1. \* $P < 0.05$ .  $n = 3$  uninfected and 5 *H. pylori* SS1 infected mice per genotype. Significance was calculated by one-way ANOVA with Newman-Keuls post-test.



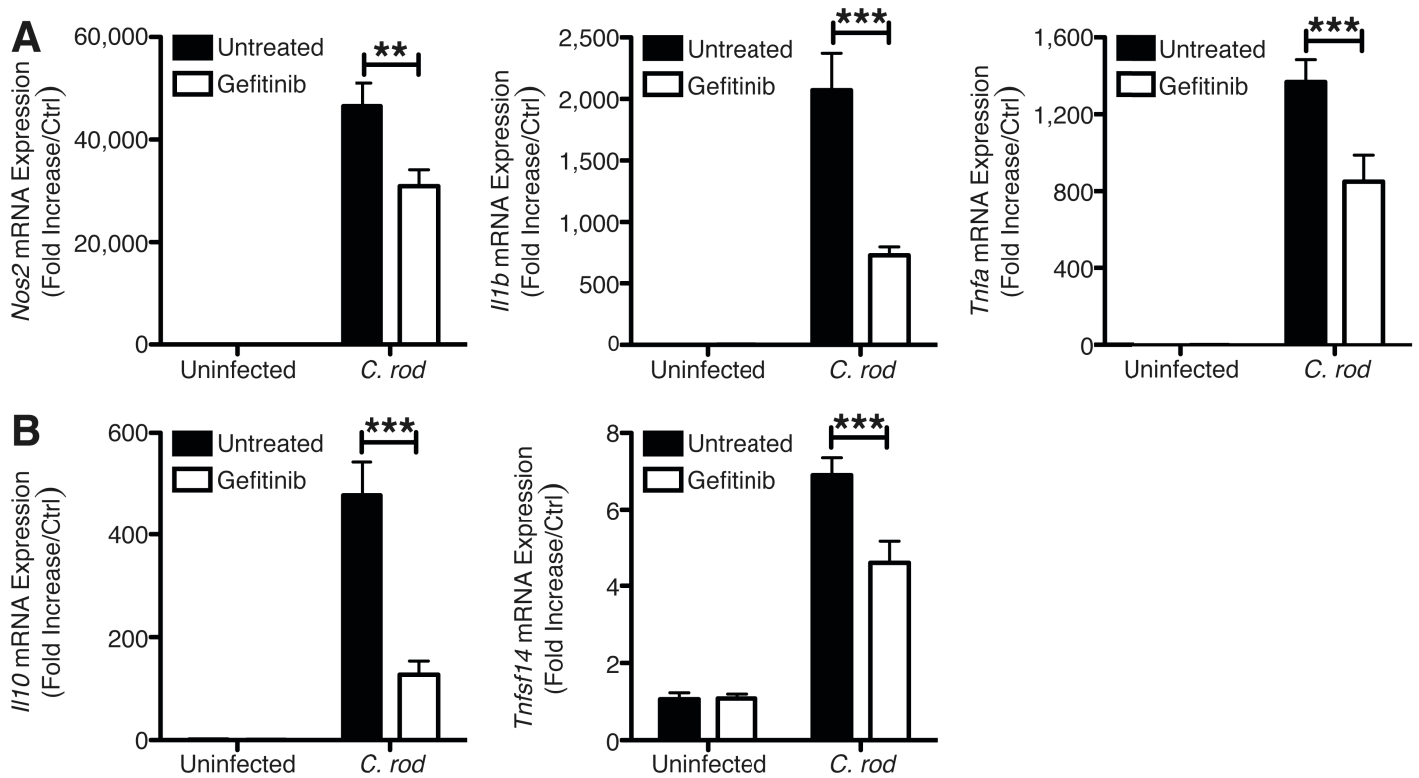
**Supplemental Figure 10. Markers of M1 activation are significantly decreased in *Egfr<sup>Δmye</sup>* colonic tissue during *C. rodentium* infection.** *Nos2*, *Tnfa*, and *Il1b* mRNA expression were assessed by RT-PCR in colonic tissue 14 d p.i. \**P* < 0.05, \*\**P* < 0.01. *n* = 5 uninfected and 7-8 *C. rodentium* infected mice per genotype. Statistical significance was calculated by one-way ANOVA with Kruskal-Wallis test, followed by Mann-Whitney *U* test.



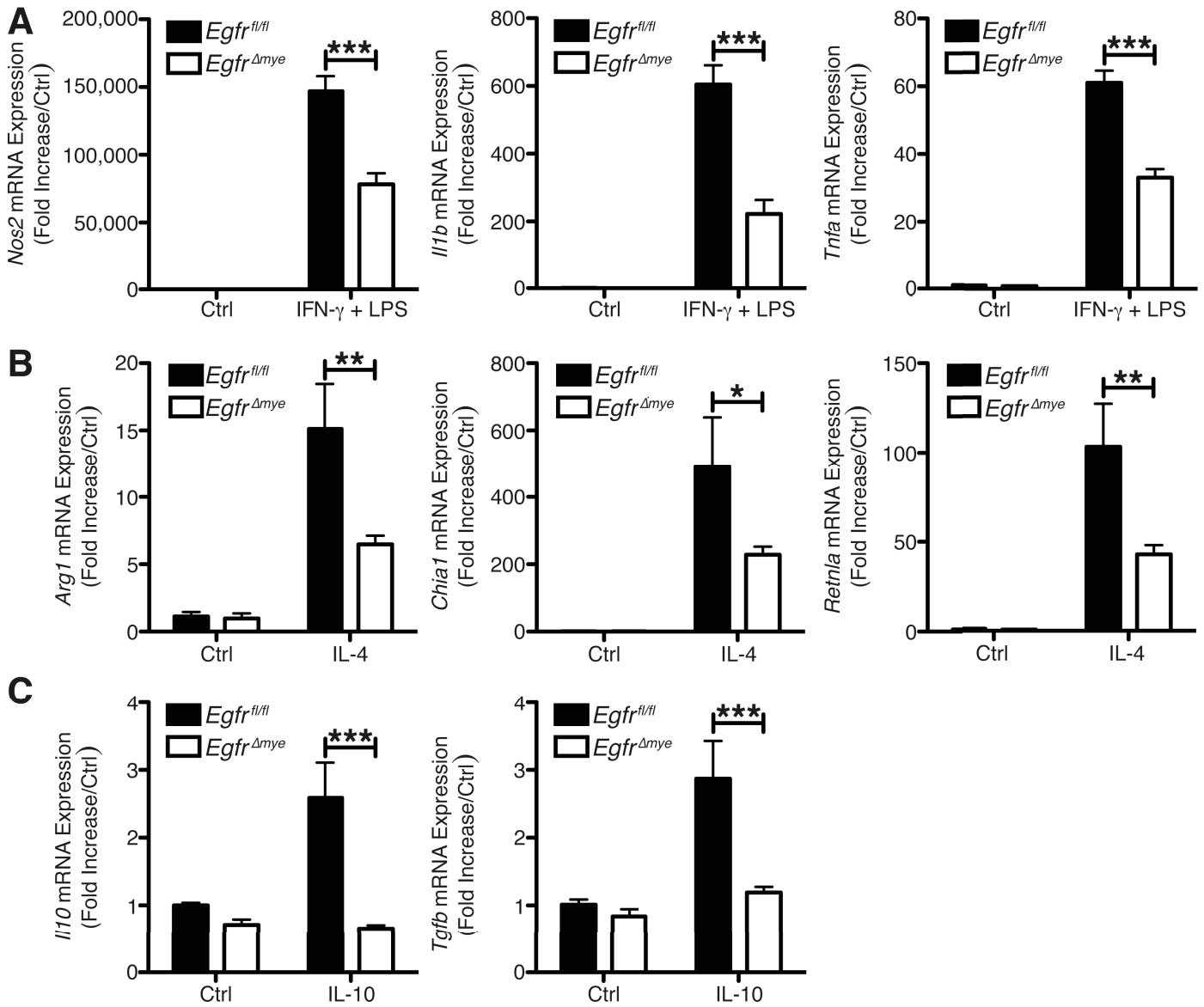
**Supplemental Figure 11. Isolation and differentiation of macrophages and dendritic cells from murine bone marrow.** (A) Representative flow cytometry scatter plots demonstrating populations of CD11b<sup>+</sup>F4/80<sup>+</sup> BMmacs. (B) Representative flow cytometry scatter plots demonstrating populations of CD11b<sup>+</sup>CD11c<sup>+</sup> bone marrow derived dendritic cells (BMDCs). In both panels,  $n = 4$  biological replicates.



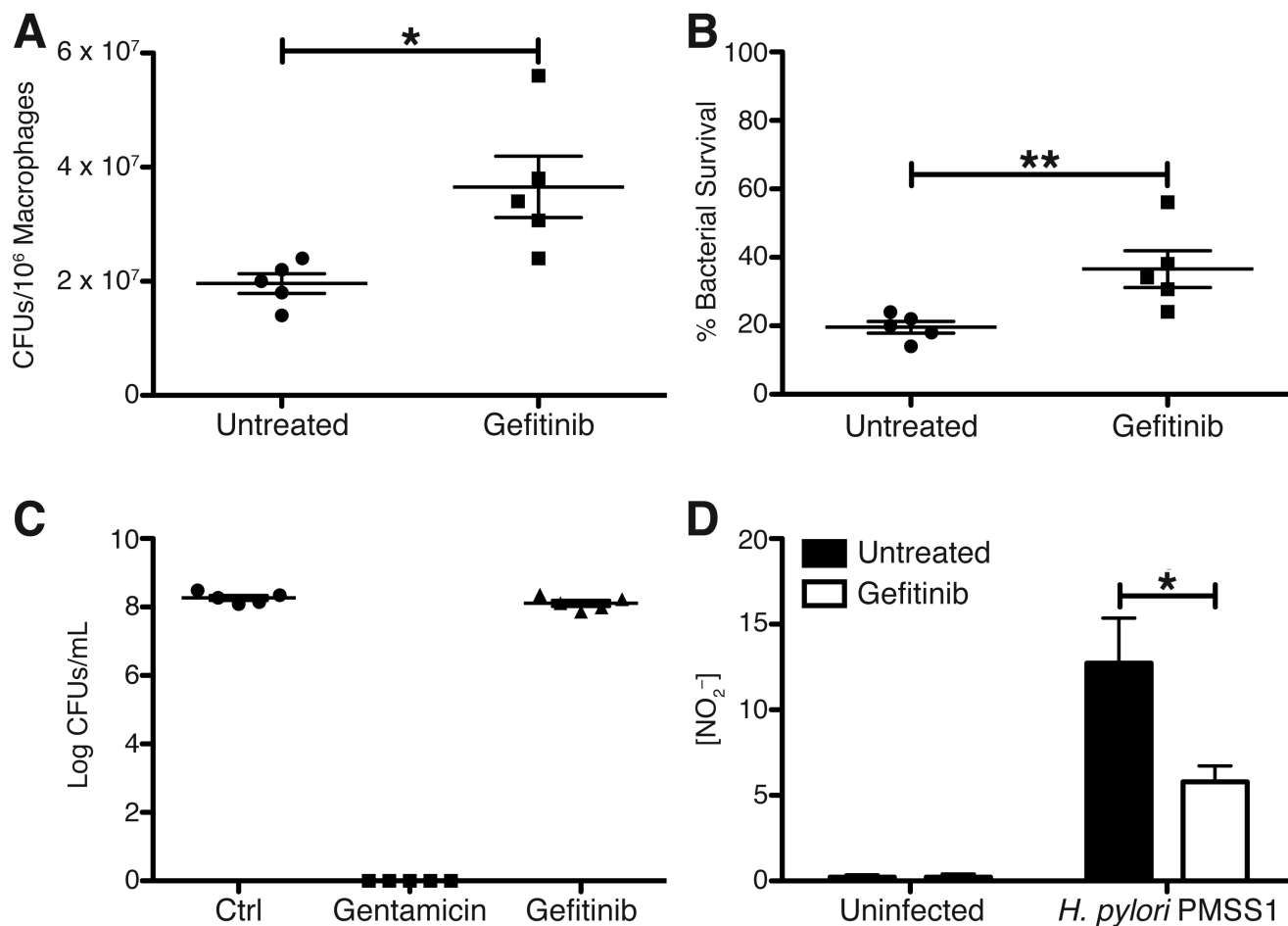
**Supplemental Figure 12. Markers of Mreg activation are significantly decreased during *H. pylori* infection, but markers of M2 activation are not significantly altered in EGFR signaling-deficient BMmacs.** (A) *I110* and *Tgfb* mRNA levels were assessed by RT-PCR in wildtype (WT) BMmacs  $\pm$  10  $\mu$ M gefitinib 24 h p.i. with *H. pylori* PMSS1. \*\* $P < 0.01$ , \*\*\* $P < 0.001$ .  $n = 4$  biological replicates. (B) *I110* and *Tgfb* mRNA levels were assessed by RT-PCR in *Egfr<sup>fl/fl</sup>* and *Egfr<sup>Δmye</sup>* BMmacs 24 h p.i. with *H. pylori* PMSS1. \*\*\* $P < 0.001$ .  $n = 4$  mice per genotype. Statistical significance in (A) and (B) was calculated by one-way ANOVA with Newman-Keuls post-test. (C) *Arg1* and *Chia1* mRNA levels were assessed by RT-PCR in WT BMmacs  $\pm$  10  $\mu$ M gefitinib 24 h p.i. with *H. pylori* PMSS1.  $n = 4$  biological replicates. (D) *Arg1* and *Chia1* mRNA levels were assessed by RT-PCR in *Egfr<sup>fl/fl</sup>* and *Egfr<sup>Δmye</sup>* BMmacs 24 h p.i. with *H. pylori* PMSS1.  $n = 4$  mice per genotype.



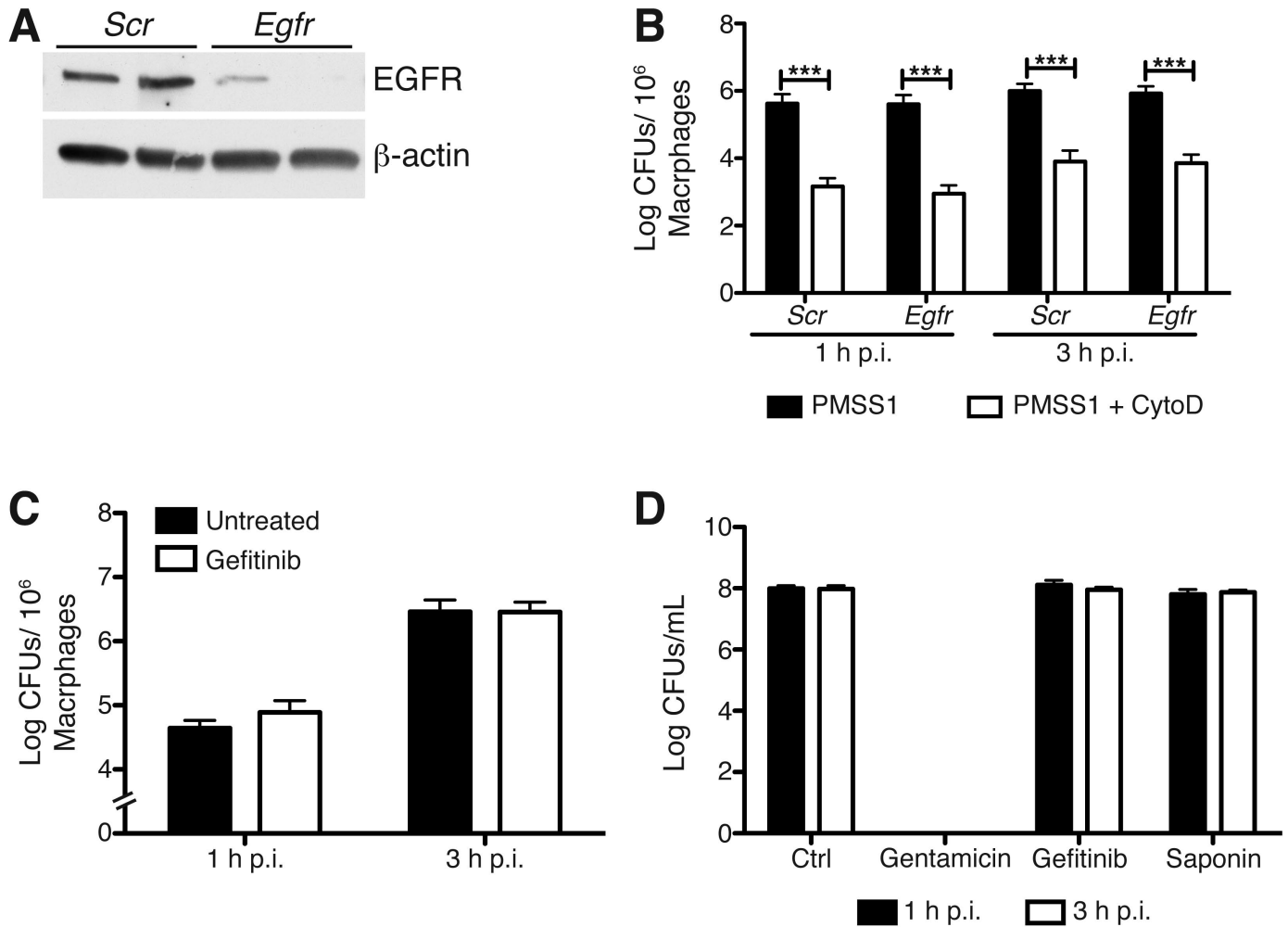
**Supplemental Figure 13. M1 and Mreg activation markers are significantly decreased in EGFR signaling-deficient BMmacs infected with *C. rodentium*.** (A) mRNA levels M1 activation markers, *Nos2*, *Il1b*, and *Tnfa*, were assessed by in WT BMmacs  $\pm$  10  $\mu$ M gefitinib 6 h p.i. by RT-PCR.  $**P < 0.01$ ,  $***P < 0.001$ .  $n = 5$  biological replicates. (B) mRNA levels Mreg activation markers, *Il10* and *Tgfb*, were assessed in WT BMmacs  $\pm$  10  $\mu$ M gefitinib 6 h p.i. by RT-PCR.  $***P < 0.001$ .  $n = 5$  biological replicates. Statistical significance in all panels was calculated by one-way ANOVA with Newman-Keuls post-test.



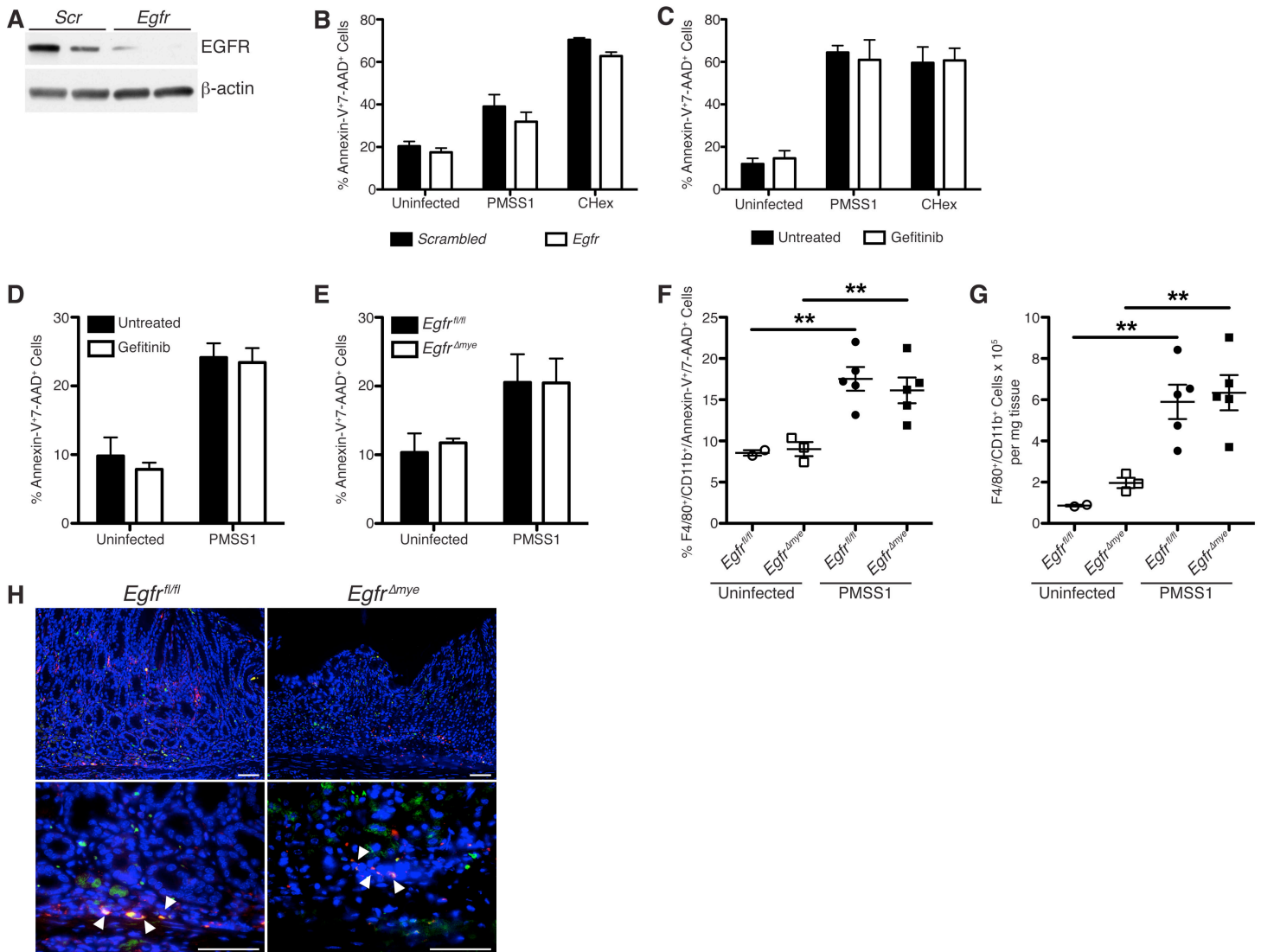
**Supplemental Figure 14. EGFR signaling regulates macrophage activation during stimulation with classical M1, M2, and Mreg activation stimuli.** (A) *Nos2*, *Il1b*, and *Tnfa* mRNA levels were assessed by RT-PCR in *Egfr<sup>fl/fl</sup>* and *Egfr $\Delta$ mye* BMmacs 24 h post stimulation with IFN- $\gamma$  (200 U/mL) and LPS (10 ng/mL). \*\*\* $P$  < 0.001.  $n$  = 3 mice per genotype. (B) *Arg1*, *Chia1*, and *Retnla* mRNA levels were assessed by RT-PCR in *Egfr<sup>fl/fl</sup>* and *Egfr $\Delta$ mye* BMmacs 24 h post stimulation with IL-4 (10 ng/mL). \* $P$  < 0.05, \*\* $P$  < 0.01.  $n$  = 3 mice per genotype. (C) *Il10* and *Tgfb* mRNA levels were assessed by RT-PCR in *Egfr<sup>fl/fl</sup>* and *Egfr $\Delta$ mye* BMmacs 24 h post stimulation with IL-10 (10 ng/mL). \*\*\* $P$  < 0.001.  $n$  = 3 mice per genotype. Statistical significance in all panels was calculated by one-way ANOVA with Newman-Keuls post-test.



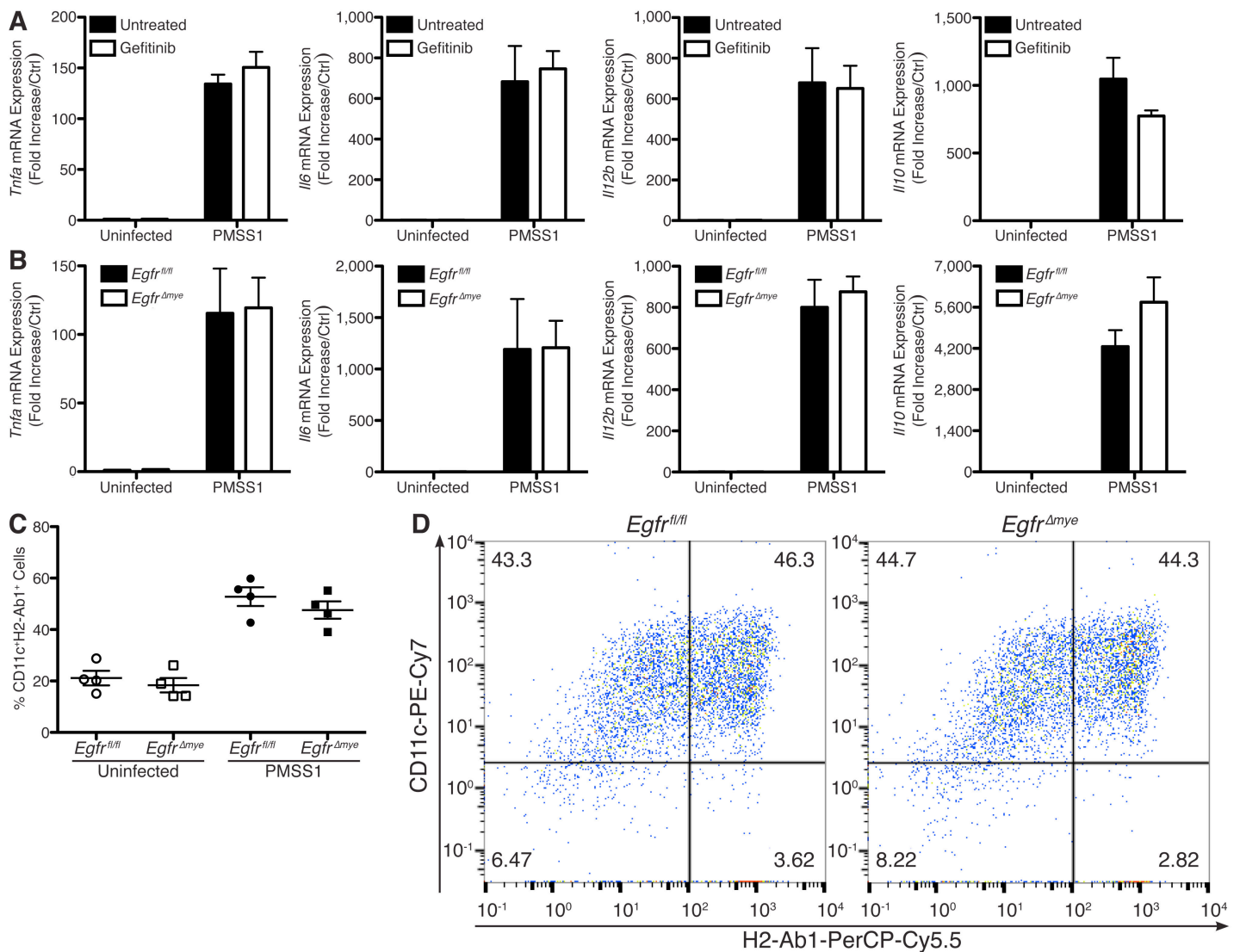
**Supplemental Figure 15. EGFR inhibition enhances bacterial survival by inhibiting NO production and NO-mediated killing.** RAW 264.7 cells and *H. pylori* PMSS1 were co-cultured across Transwell filter supports for 24 h. (A) *H. pylori* survival was assessed by serial dilution and culture from Transwell filter supports above RAW 264.7 cells  $\pm$  10  $\mu$ M gefitinib. \* $P$  < 0.05.  $n$  = 5 biological replicates. (B) Percent of bacteria that survived NO-mediated killing based on the initial MOI of 100 and the bacteria cultured in (A). \*\* $P$  < 0.01.  $n$  = 5 biological replicates. Statistical significance in (A) and (B) was calculated by Student's  $t$  test. (C) A set of control conditions for these assays. Culture of *H. pylori* PMSS1 in DMEM + 10% FBS does not result in bacterial death. Gentamicin treatment served as a positive control, leading to 100% bacterial death. Treatment of *H. pylori* PMSS1 with 10  $\mu$ M gefitinib did not result in bacterial death.  $n$  = 5 biological replicates. (D) Measurement of NO<sub>2</sub><sup>-</sup> from RAW 264.7 cell supernatants  $\pm$  10  $\mu$ M gefitinib 24 h p.i. with *H. pylori* PMSS1. \* $P$  < 0.05.  $n$  = 5 biological replicates. Statistical significance was calculated by one-way ANOVA with Newman-Keuls post-test.



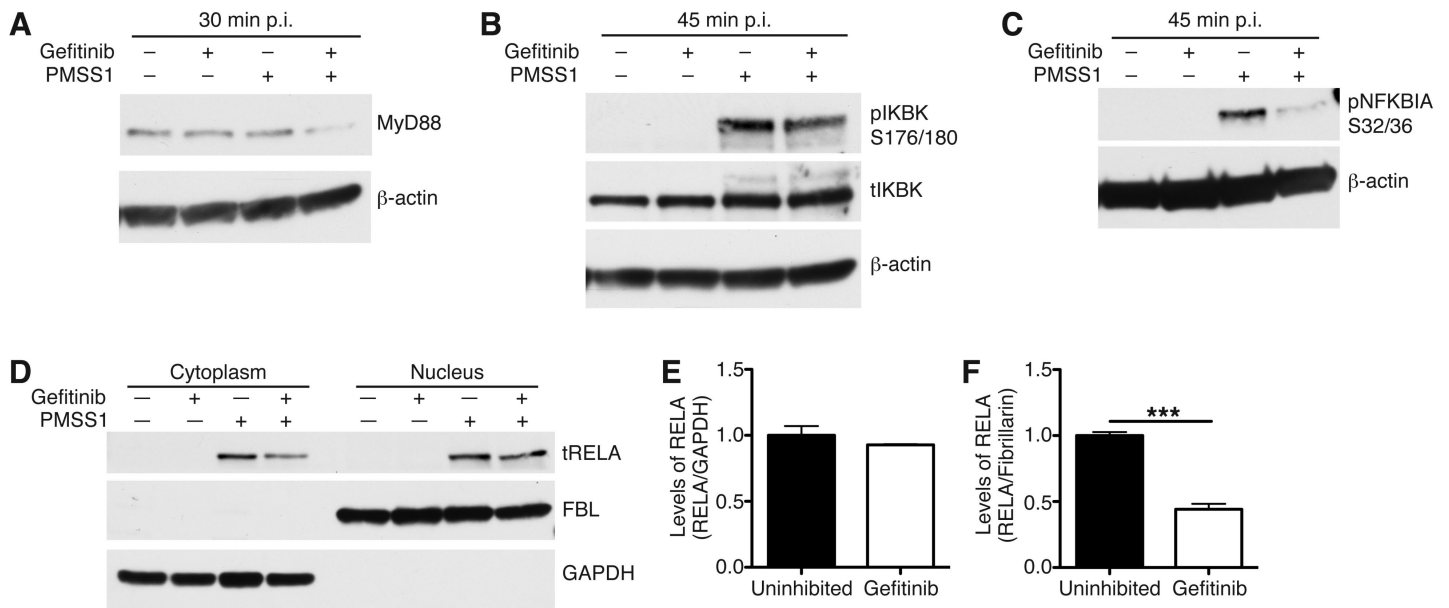
**Supplemental Figure 16. EGFR inhibition cells does not affect phagocytosis of *H. pylori* PMSS1.** (A) Confirmation of *Egfr* knockdown by siRNA in RAW 264.7 cells by western blot.  $n = 2$  biological replicates. (B) The amount of *H. pylori* PMSS1 that was phagocytosed by RAW 264.7 cells  $\pm$  10  $\mu$ M cytochalasin D (CytoD) at 1 h and 3 h p.i. was assessed by serial dilution and culture.  $***P < 0.001$ . Statistical significance was calculated by one-way ANOVA with Newman-Keuls post-test.  $n = 3$  biological replicates. Scr = scrambled siRNA. *Egfr* = *Egfr* siRNA. (C) The amount of *H. pylori* that was phagocytosed by RAW 264.7 cells  $\pm$  10  $\mu$ M gefitinib at 1 h and 3 h p.i. was assessed by serial dilution and culture.  $n = 3$  biological replicates. (D) Confirmation that gentamicin treatment (200  $\mu$ g/mL) for 30 min kills >99% of *H. pylori* PMSS1 and that 10  $\mu$ M gefitinib treatment for 1 h and 0.1% saponin treatment for 30 min kills <1% of *H. pylori* PMSS1.  $n = 3$  biological replicates.



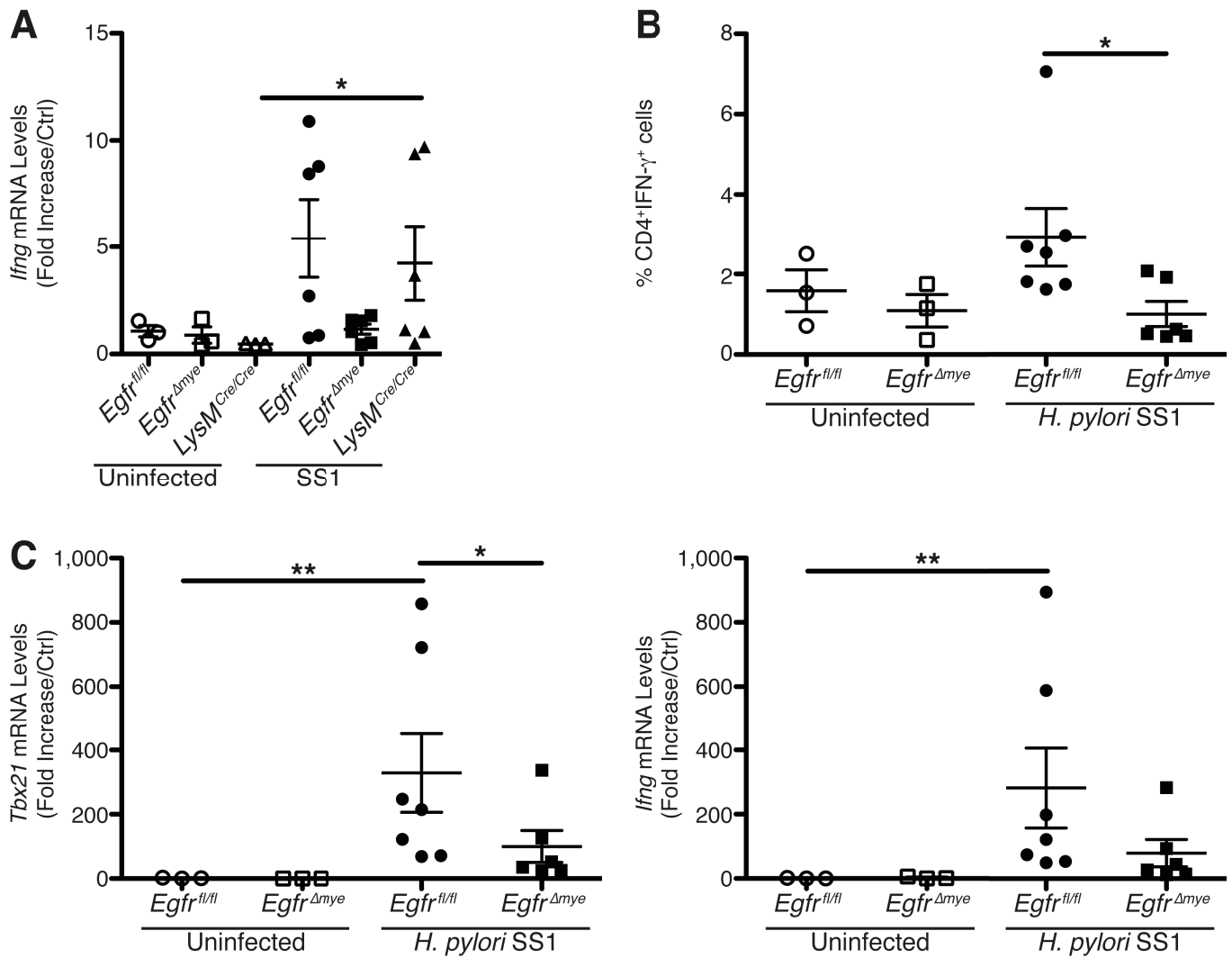
**Supplemental Figure 17. EGFR knockdown or inhibition does not affect apoptosis of macrophages during *H. pylori* PMSS1 infection.** (A) Confirmation of *Egfr* knockdown by siRNA in RAW 264.7 cells by western blot.  $n = 2$  biological replicates. (B) Percentage of Annexin-V7-AAD<sup>+</sup> RAW 264.7 cells  $\pm$  *Egfr* siRNA knockdown 24 h p.i. with *H. pylori* PMSS1.  $n = 3$  biological replicates. CHex = cyclohexamide (5  $\mu$ g/mL). (C) Percentage of Annexin-V7-AAD<sup>+</sup> RAW 264.7 cells  $\pm$  10  $\mu$ M gefitinib 24 h p.i. with *H. pylori* PMSS1.  $n = 3$  biological replicates. CHex = cyclohexamide (5  $\mu$ g/mL). (D) Percentage of Annexin-V7-AAD<sup>+</sup> WT BMmacs  $\pm$  10  $\mu$ M gefitinib 24 h p.i. with *H. pylori* PMSS1.  $n = 3$  biological replicates. (E) Percentage of Annexin-V7-AAD<sup>+</sup> *Egfr*<sup>fl/fl</sup> and *Egfr* <sup>$\Delta$ mye</sup> BMmacs 24 h p.i. with *H. pylori* PMSS1.  $n = 3$  biological replicates. (F) Percentage of F4/80<sup>+</sup>CD11b<sup>+</sup>Annexin-V7-AAD<sup>+</sup> Gmacs from *Egfr*<sup>fl/fl</sup> and *Egfr* <sup>$\Delta$ mye</sup> mice 48 h p.i. with *H. pylori* SS1. **\*\*** $P < 0.01$ .  $n = 3$  uninfected and 5 *H. pylori* PMSS1 infected mice per genotype. (G) Number of F4/80<sup>+</sup>CD11b<sup>+</sup> Gmacs from *Egfr*<sup>fl/fl</sup> and *Egfr* <sup>$\Delta$ mye</sup> mice 48 h p.i. with *H. pylori* SS1. **\*\*** $P < 0.01$ .  $n = 3$  uninfected and 5 *H. pylori* PMSS1 infected mice per genotype. Statistical significance in (F)-(G) was calculated by one-way ANOVA with Newman-Keuls post-test. (H) Representative immunofluorescence images of cleaved caspase 3 staining in *Egfr*<sup>fl/fl</sup> and *Egfr* <sup>$\Delta$ mye</sup> gastric tissues 4 mo p.i. with *H. pylori* SS1. Green = cleaved caspase 3, Red = CD68, Yellow = merge, Blue = DAPI. Arrows indicate CD68<sup>+</sup>cleaved caspase 3<sup>+</sup> macrophages. Scale bars = 50  $\mu$ M.  $n \geq 3$  mice per genotype.



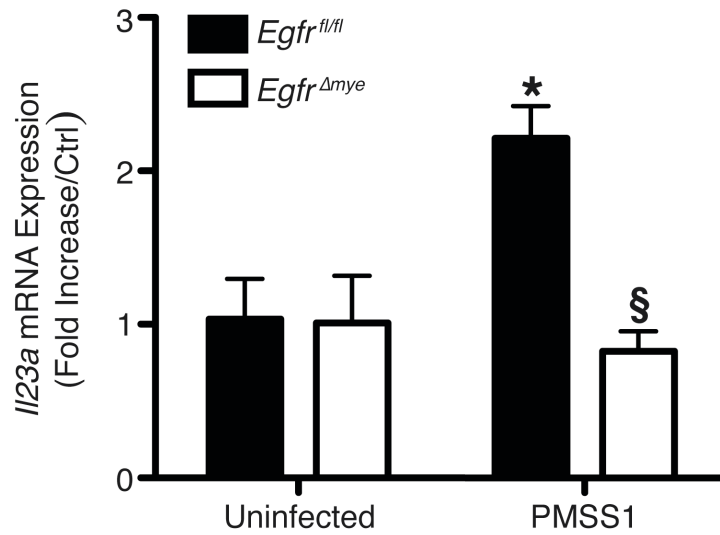
**Supplemental Figure 18. EGFR inhibition or knockout does not affect cytokine production or antigen presentation by bone marrow-derived dendritic cells.** (A) mRNA levels of prototypical dendritic cell cytokines, *Tnfa*, *Il6*, *Il12b* (*Il12p40*), and *Il10*, were assessed by RT-PCR 24 h p.i. with *H. pylori* PMSS1 in WT BMDCs  $\pm$  10  $\mu$ M gefitinib.  $n = 4$  biological replicates. (B) mRNA levels of prototypical dendritic cell cytokines, *Tnfa*, *Il6*, *Il12b*, and *Il10*, were assessed by RT-PCR 24 h p.i. with *H. pylori* PMSS1 in *Egfr<sup>fl/fl</sup>* and *Egfr<sup>Δmye</sup>* BMDCs.  $n = 4$  mice per genotype. (C) Antigen presentation ability was assessed by determining levels of surface H2-Ab1 (MHCI) on *Egfr<sup>fl/fl</sup>* and *Egfr<sup>Δmye</sup>* CD11c<sup>+</sup> BMDCs 24 h p.i. with *H. pylori* PMSS1.  $n = 4$  biological replicates. (D) Representative flow cytometry scatter plots for *H. pylori*-infected *Egfr<sup>fl/fl</sup>* and *Egfr<sup>Δmye</sup>* BMDCs from (C).  $n = 4$  biological replicates.



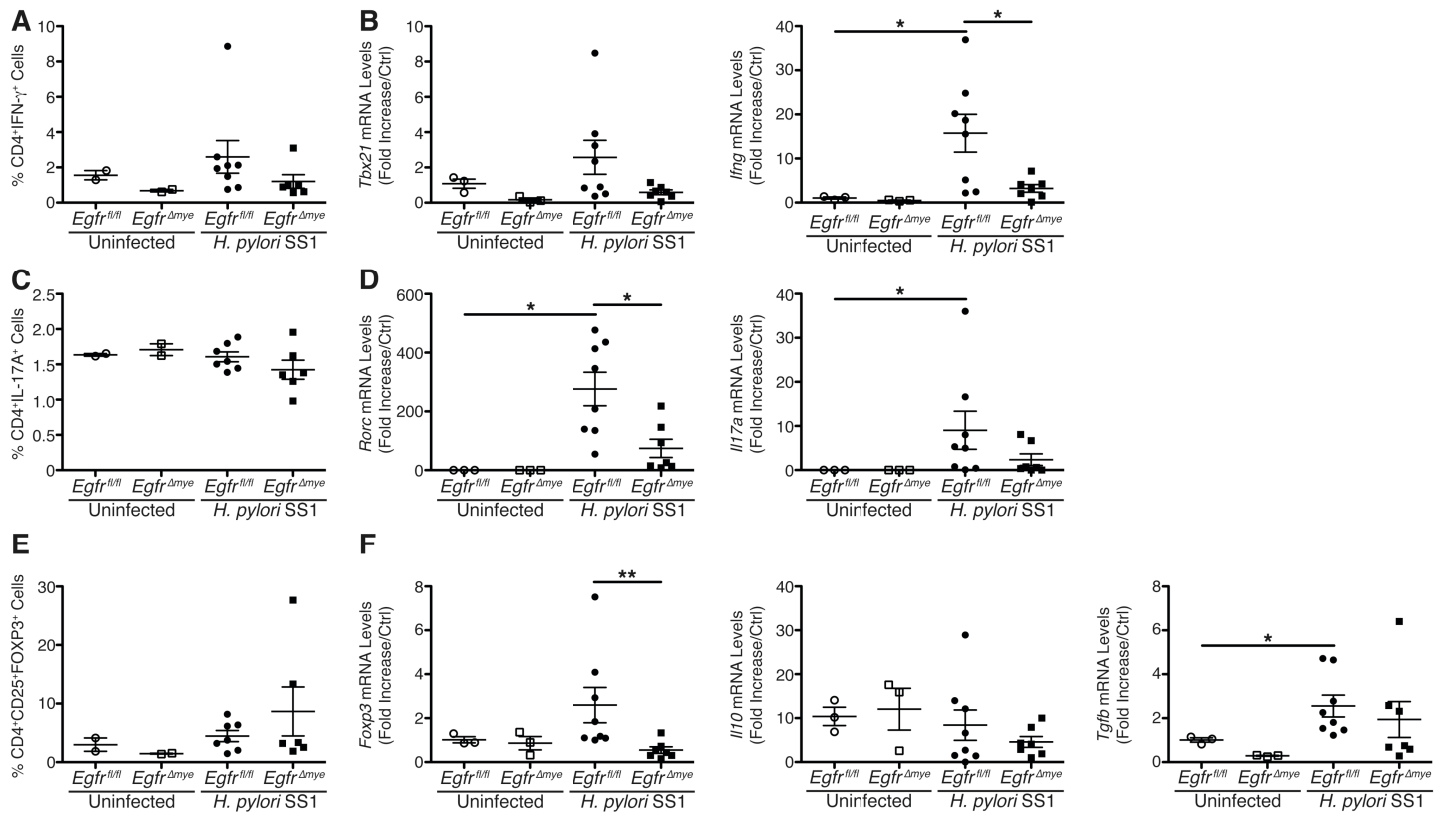
**Supplemental Figure 19. EGFR inhibition leads to markedly decreased NF- $\kappa$ B signaling.** (A) Representative western blot of MyD88 protein levels in WT BMmacs  $\pm$  10  $\mu$ M gefitinib.  $n = 3$  biological replicates. (B) Representative western blot of pIKBK (pIKK) and tIKBK (tIKK) protein levels in WT BMmacs  $\pm$  10  $\mu$ M gefitinib.  $n = 3$  biological replicates. (C) Representative western blot of pNF $\kappa$ BIA (pI $\kappa$ B) protein levels in WT BMmacs  $\pm$  10  $\mu$ M gefitinib.  $n = 3$  biological replicates. (D) Representative western blot of tRELA (p65) protein levels in the cytoplasm and nucleus of WT BMmacs  $\pm$  10  $\mu$ M gefitinib.  $n = 3$  biological replicates. (E) Densitometric analysis of tRELA protein levels the cytoplasm in (D)  $n = 3$  biological replicates. (F) Densitometric analysis of tRELA levels in the nucleus in (D). \*\*\* $P < 0.001$ .  $n = 3$  biological replicates. Statistical significance was calculated by Student's  $t$  test.



**Supplemental Figure 20. Macrophage EGFR signaling has a modest effect on the Th1 response to *H. pylori* 4 mo p.i.** (A) *Ifng* mRNA expression was assessed by RT-PCR in *Egfr<sup>fl/fl</sup>*, *Egfr<sup>Δmye</sup>*, and *LysM<sup>Cre/Cre</sup>* gastric tissues 4 mo p.i. with *H. pylori* SS1. \* $P < 0.05$ .  $n = 3$  uninfected and 6 *H. pylori* SS1 infected mice per genotype. (B) Assessment of CD4<sup>+</sup>IFN-γ<sup>+</sup> T cells from gastric lymph nodes (GLN) of *Egfr<sup>fl/fl</sup>* and *Egfr<sup>Δmye</sup>* mice 4 mo p.i. by flow cytometry. Isolated T cells were cultured in 96-well plates containing 5 μg/mL anti-CD3 and 1 μg/mL anti-CD28. Cells were then stimulated with 20 ng/mL PMA and 1 μg/mL ionomycin for 4 h. \* $P < 0.05$ .  $n = 3$  uninfected and 6-7 *H. pylori* SS1 infected mice per genotype. (C) *Tbx21* (*Tbet*) and *Ifng* mRNA expression was assessed by RT-PCR from magnetically selected CD4<sup>+</sup> T cells from the gastric lamina propria of *Egfr<sup>fl/fl</sup>* and *Egfr<sup>Δmye</sup>* mice 4 mo p.i. \* $P < 0.05$ , \*\* $P < 0.01$ .  $n = 3$  uninfected and 6-7 *H. pylori* SS1 infected mice per genotype. Statistical significance in all panels was calculated by one-way ANOVA with Kruskal-Wallis test, followed by Mann-Whitney *U* test.



**Supplemental Figure 21. Macrophage EGFR signaling results in *IL23a* expression in gastric tissues and primary macrophages in response to *H. pylori*.** *IL23a* (*IL23p19*) mRNA expression was assessed by RT-PCR in *Egfr<sup>fl/fl</sup>* and *Egfr<sup>Δmye</sup>* BMmacs 24 h p.i. with *H. pylori* PMSS1. \* $P < 0.05$  vs. *Egfr<sup>fl/fl</sup>* control BMmacs. § $P < 0.05$  vs. PMSS1-infected *Egfr<sup>fl/fl</sup>* BMmacs.  $n = 4$  mice per genotype. Statistical significance in all panels was calculated by one-way ANOVA with Newman-Keuls post-test.



**Supplemental Figure 22. Macrophage EGFR signaling has a modest effect on Th1, Th17, and Treg responses to *H. pylori* 2 mo p.i.** (A) Assessment of CD4<sup>+</sup>IFN- $\gamma$ <sup>+</sup> T cells from GLNs of *Egfr<sup>fl/fl</sup>* and *Egfr<sup>Δmye</sup>* mice 4 mo p.i. by flow cytometry. Isolated T cells were cultured in 96-well plates containing 5  $\mu$ g/mL anti-CD3 and 1  $\mu$ g/mL anti-CD28. Cells were then stimulated with *H. pylori* French-pressed lysate for 4 h. \* $P$  < 0.05. (B) *Tbx21* (*Tbet*) and *Irfg* mRNA expression was assessed by RT-PCR from magnetically selected CD4<sup>+</sup> T cells from the gastric lamina propria of *Egfr<sup>fl/fl</sup>* and *Egfr<sup>Δmye</sup>* mice 4 mo p.i. \* $P$  < 0.05, \*\* $P$  < 0.01. (C) Assessment of CD4<sup>+</sup>IL-17<sup>+</sup> T cells from GLNs of *Egfr<sup>fl/fl</sup>* and *Egfr<sup>Δmye</sup>* mice 4 mo p.i. by flow cytometry. Cells isolated and stimulated as in (A). (D) *Rorc* (*Roryt*) and *I17a* mRNA expression was assessed by RT-PCR from magnetically-selected CD4<sup>+</sup> T cells from the gastric lamina propria of *Egfr<sup>fl/fl</sup>* and *Egfr<sup>Δmye</sup>* mice 4 mo p.i. \* $P$  < 0.05. (E) Assessment of CD4<sup>+</sup>CD25<sup>+</sup>FOXP3<sup>+</sup> T cells from GLNs of *Egfr<sup>fl/fl</sup>* and *Egfr<sup>Δmye</sup>* mice 4 mo p.i. by flow cytometry. Cells isolated and stimulated as in (A). (F) *Foxp3*, *I110*, and *Tgfb* mRNA expression was assessed by RT-PCR from magnetically selected CD4<sup>+</sup> T cells from the gastric lamina propria of *Egfr<sup>fl/fl</sup>* and *Egfr<sup>Δmye</sup>* mice 4 mo p.i. \* $P$  < 0.05, \*\* $P$  < 0.01. In all panels,  $n$  = 2-3 uninfected and 6-8 *H. pylori* SS1 infected mice per genotype. Statistical significance in all panels was calculated by one-way ANOVA with Kruskal-Wallis test, followed by Mann-Whitney  $U$  test.

## **Supplemental Methods**

### **Materials**

Cytocholasin D, an inhibitor of actin polymerization was obtained from EMD Millipore (Billerica, MA, USA). ON-TARGET<sub>plus</sub> siRNA against *Egfr*, and scrambled targets were purchased from Dharmacon (Lafayette, CO, USA).

### **Bacteria, Cells, Culture Conditions and, Infections**

*Citrobacter rodentium* was cultured as previously described (1). Cells were infected at an MOI of 10 for all experiments with *C. rodentium*.

### **Transfections**

RAW 264.7 cells in Opti-MEM I Reduced Serum Media were transfected using Lipofectamine 2000 (Invitrogen, Carlsbad, CA, USA) with 100 nM ON-TARGET<sub>plus</sub> siRNAs directed against *Egfr*, and scrambled targets. After 6 h, the cells were washed and then maintained for 36 h in serum-containing, antibiotic-free DMEM. Cells were then stimulated as described in the “Bacteria, Cells, Culture Conditions, and Infections” section of the Methods.

### **Animal Studies**

For the colitis studies, the same sex and age requirements utilized for *H. pylori* experiments were applied to the mice. Moreover, samples sizes were based on previous studies in our laboratory (1-3). Mice were infected orogastrically with  $5 \times 10^8$  CFUs once for all studies with *C. rodentium*. Animals were weighed daily and sacrificed 14 days post-infection. Colonization was assessed by serial dilution and culture. Histology was assessed in a completely blinded manner by M. Blanca Piazuelo, as previously described (2, 3).

### **Measurement of NO-mediated Bacterial Killing**

RAW 264.7 cells were plated in complete DMEM in 24 well plates and allowed to adhere. Cells were then washed and placed in complete DMEM, without antibiotics. Transwell filter supports were placed over the cells. *H. pylori* PMSS1 (MOI = 100) were then placed in the Transwell filter supports above the cells for 24 h. After 24

h, bacteria in the Transwells were quantified by serial dilution and culture. NO was measured by the Griess Reaction, described in the Methods, from the supernatants below the Transwell filter supports.

### **Measurement of Phagocytosis**

Phagocytosis was measured by gentamicin protection assay as previously published (4).

### **Immunohistochemistry**

Immunohistochemistry was performed on gastric biopsies from the Vanderbilt University TMA. Paraffin-embedded tissues were deparaffinized, antigen retrieval was performed, and tissues were stained for pEGFR as previously described (5). See **Supplemental Table 3** for antibody information.

### **Quantification of Human TMA Immunofluorescence**

The TMA was analyzed using CellProfiler (<http://www.cellprofiler.org>) software. Analysis was performed on images from the Ariol SL-50 platform (Leica Biosystems, Buffalo Grove, IL, USA). A CellProfiler pipeline was created that identified nuclei, CD68<sup>+</sup> cells and pEGFR<sup>+</sup> cells based on size and staining intensity. CD68<sup>+</sup>pEGFR<sup>+</sup> cells were determined by the overlap of the CD68 and pEGFR staining, measured in pixels. All cells were required to have a nucleus to be counted in the analysis, thus eliminating red blood cells and non-specific staining. A serial section of the TMA was concurrently stained with hematoxylin and eosin (H&E) and histologic diagnosis was confirmed in order to ensure that only high quality cores were included in the analysis described in this section. Samples were excluded from this analysis if histologic diagnosis could not be made due to sample degradation.

### **Apoptosis**

Apoptosis was assayed using Annexin-V/7-AAD as previously published (6).

## NF- $\kappa$ B Reporter Assay

The NF- $\kappa$ B reporter assay was performed as previously published (7, 8). In brief, NGL cells were pre-treated with 10  $\mu$ M gefitinib for 1 h and then infected with *H. pylori* PMSS1 and SS1 at MOI = 100 for 2, 3 and 4 h. Luciferase activity was assessed using the Luciferase Assay System kit (Promega, Madison, WI, USA).

## Luminex Assay

A 32-plex assay (EMD Millipore, Cat. MCYTMAG-70K-PX32, Billerica, MA, USA) was performed on gastric tissues from uninfected and infected *Egfr*<sup>fl/fl</sup>, *Egfr* <sup>$\Delta$ mye</sup> and *LysM*<sup>cre/cre</sup> mice. Protein isolation, quantification and Luminex assay were performed as previously described (9).

## Flow Cytometry for F4/80, CD11b, and tEGFR in Gmcs

Lamina propria cells were isolated from the stomach at 48 h p.i. with *H. pylori* SS1, as described (6). Upon isolation, the cells were fixed and permeabilized with CytoFix/CytoPerm (BD Biosciences, Cat. No. 554714) for 20 min on ice. Following fixation and permeabilization, cells were washed 3 times with BD CytoFix/CytoPerm and then stained with a polyclonal rabbit anti-total EGFR antibody at 1:50 (Cell Signaling Technologies, Cat. No. 2232), or a general rabbit IgG isotype control at 1:50 (Jackson ImmunoResearch, Cat. No. 111-095-003), for 1 h on ice in BD CytoFix/CytoPerm. Cells were washed 3 times with BD CytoFix/CytoPerm and then stained for F4/80-PE (1:100, Invitrogen, Cat. No. MF48004), CD11b-PE-Cy7 (1:100, BD Biosciences, Cat. No. 552850), and anti-rabbit-Alexa488 (1:200, Jackson ImmunoResearch, Cat. No. 111-095-003) for 20 min on ice in flow cytometry staining buffer solution (eBiosciences, Cat. 04-4222-26). Upon completion of staining, cells were washed 3 times in flow cytometry staining buffer solution and subsequently analyzed utilizing flow cytometry. See **Supplemental Table 3** for further antibody information.

## T Cell Studies

Single-cell suspensions from perigastric lymph nodes (GLN) of uninfected and *H. pylori* SS1 infected *Egfr*<sup>fl/fl</sup> and *Egfr* <sup>$\Delta$ mye</sup> mice were cultured in Roswell Park Memorial Institute medium (RPMI) with 10% FBS, 10 mM HEPES, 100 U/mL penicillin, 100  $\mu$ g/mL streptomycin, and 10  $\mu$ g/mL gentamicin in 96-well plates coated with 5

$\mu\text{g}/\text{mL}$  anti-CD3 and  $1 \mu\text{g}/\text{mL}$  anti-CD28. Cells were stimulated with  $20 \text{ ng}/\text{mL}$  PMA and  $1 \mu\text{g}/\text{mL}$  ionomycin for 4 h. Cells were then stained and assayed by flow cytometry, as described below. Cells from GLN utilized for assessing Treg populations were not cultured, and were stained directly upon isolation.

$\text{CD4}^+$  cells from the gastric lamina propria were purified utilizing the protocol for isolation and purification of Gmacs. Lamina propria cells were incubated in the presence of a 1:100 dilution of anti-CD4, biotin tagged antibody (BD Biosciences, San Diego, CA) for 1 h, followed by incubation with  $100 \mu\text{L}$  streptavidin-conjugated iMag beads (BD Biosciences, San Diego, CA) for 1 h.  $\text{CD4}^+$  cells were then magnetically selected and RNA isolated utilizing the 5 PRIME PerfectPure 96 CS Cell RNA kit (5 PRIME, Gaithersburg, MD) and cDNA synthesized as described above. Th1, Th17, and Treg genes were then assessed by RT-PCR. See **Supplemental Table 2** for primer information.

Analyte	Concentration of Analyte (pg/mg protein); Mean ± S.E.M.					
	<i>Egfr<sup>fl/fl</sup></i>		<i>Egfr<sup>Δmye</sup></i>		<i>LysM<sup>Cre/Cre</sup></i>	
	Uninfected	<i>H. pylori</i> SS1	Uninfected	<i>H. pylori</i> SS1	Uninfected	<i>H. pylori</i> SS1
CCL2	4.10 ± 1.70	24.20 ± 6.78 *	14.26 ± 3.98	16.14 ± 4.21	15.59 ± 1.01	26.08 ± 4.75
CCL11	50.62 ± 9.20	47.73 ± 6.00	54.40 ± 2.95	47.32 ± 4.33	41.25 ± 4.79	59.80 ± 7.42
CSF1	2.83 ± 0.49	4.69 ± 0.31	2.85 ± 0.37	4.08 ± 0.44	4.50 ± 1.81	3.62 ± 0.37
CSF2	1.21 ± 0.54	0.74 ± 0.16	1.73 ± 0.88	1.18 ± 0.59	1.42 ± 1.15	2.55 ± 0.93
CSF3	4.29 ± 0.60	8.54 ± 1.56	4.54 ± 0.89	5.68 ± 0.62	4.42 ± 1.19	8.19 ± 0.70
IFN-γ	2.63 ± 0.45	4.57 ± 1.21	2.90 ± 0.31	2.68 ± 0.30	2.61 ± 0.04	3.38 ± 0.38
IL-1α	48.07 ± 6.10	38.85 ± 5.73	44.49 ± 5.58	43.36 ± 5.05	35.06 ± 3.76	42.53 ± 5.07
IL-1β	4.21 ± 1.23	9.75 ± 1.72 *	4.96 ± 1.36	7.20 ± 1.30	9.01 ± 2.27	10.37 ± 1.19
IL-2	2.63 ± 0.42	2.78 ± 0.27	2.53 ± 0.27	2.22 ± 0.32	2.57 ± 0.14	2.62 ± 0.19
IL-6	0.70 ± 0.38	1.33 ± 0.36	0.91 ± 0.19	1.13 ± 0.24	0.70 ± 0.35	1.58 ± 0.26
IL-7	0.97 ± 0.19	1.85 ± 0.35	1.73 ± 0.39	1.20 ± 0.30	1.74 ± 0.36	2.28 ± 0.21
IL-9	0.36 ± 0.25	15.24 ± 2.82 ***	0.51 ± 0.25	4.75 ± 1.89 §	0.34 ± 0.13	26.17 ± 10.92
IL-10	3.25 ± 0.52	3.23 ± 0.50	4.84 ± 0.80	3.42 ± 0.79	4.31 ± 1.40	5.05 ± 1.47
IL-12p40	0.16 ± 0.06	0.34 ± 0.11	0.29 ± 0.05	0.13 ± 0.02 <sup>A</sup>	0.27 ± 0.07	0.38 ± 0.05 <sup>⌘⌘</sup>
IL-12p70	11.33 ± 2.94	12.95 ± 3.59	8.12 ± 3.31	9.20 ± 1.09	11.72 ± 0.24	11.40 ± 1.08
IL-15	5.29 ± 2.09	7.09 ± 1.53	5.22 ± 2.13	3.93 ± 0.90	6.51 ± 1.53	7.75 ± 0.58
IL-17	0.98 ± 0.18	4.94 ± 0.49 **	1.33 ± 0.25	3.03 ± 0.78	0.89 ± 0.14	5.51 ± 1.16
TNF-α	1.22 ± 0.23	3.10 ± 1.13	1.49 ± 0.20	1.44 ± 0.18	1.65 ± 0.05	2.70 ± 0.45
VEGFA	3.23 ± 0.31	4.47 ± 0.60	4.11 ± 0.82	3.71 ± 0.22	2.98 ± 0.19	4.24 ± 0.33

Analyses Not Detected: CXCL2, IL-3, IL-4, IL-5, IL-13, LIF, LIX

**Supplemental Table 1. Luminex analytes that did not demonstrate significant differences in gastric tissue between *Egfr<sup>fl/fl</sup>*, *Egfr<sup>Δmye</sup>* and *LysM<sup>Cre/Cre</sup>* mice.** 32 distinct analytes were assessed in gastric tissue from uninfected and infected mice from each of the three genotypes. Listed are the analytes that showed no significant differences as a result of infection, no significant differences between genotypes or were not detected. *Egfr<sup>fl/fl</sup>*: *n* = 5 uninfected, 11 infected. *Egfr<sup>Δmye</sup>*: *n* = 3 uninfected, 8 infected. *LysM<sup>Cre/Cre</sup>*: *n* = 2 uninfected, 9 infected. \* *P* < 0.05, \*\* *P* < 0.01 \*\*\* *P* < 0.001 vs. *Egfr<sup>fl/fl</sup>* Uninfected. § *P* < 0.05 vs. *Egfr<sup>fl/fl</sup>* *H. pylori* SS1. ⌘⌘ *P* < 0.01 for. *LysM<sup>Cre/Cre</sup>* *H. pylori* SS1 vs *Egfr<sup>Δmye</sup>* *H. pylori* SS1. Statistical significance was calculated by one-way ANOVA with Kruskal-Wallis test, followed by Mann-Whitney *U* test. <sup>A</sup>*P* = 0.07 between *Egfr<sup>fl/fl</sup>* *H. pylori* SS1 and *Egfr<sup>Δmye</sup>* *H. pylori* SS1.

Species	Target	Sequence
Mouse	<i>β-actin</i>	F: CCAGAGCAAGAGAGGTATCC
		R: CTGTGGTGGTGAAGCTGTAG
Mouse	<i>Nos2</i>	F: CACCTTGGAGTTCACCCAGT
		R: ACCACTCGTACTTGGGATGC
Mouse	<i>Tnfa</i>	F: CTGTGAAGGGAATGGGTGTT
		R: GGTCAGTGTCCCAGCATCTT
Mouse	<i>Il1b</i>	F: ACCTGCTGGTGTGTGACGTTCC
		R: GGGTCCGACAGCACGAGGCT
Mouse	<i>Arg1</i>	F: AAGAAAAGGCCGATTACCT
		R: CACCTCCTCTGCTGTCTTCC
Mouse	<i>Chia1</i>	F: ACTTTGATGGCCTCAACCTG
		R: AATGATTCCTGCTCCTGTGG
Mouse	<i>Retnla</i>	F: GGGATGACTGCTACTGGGTG
		R: TCAACGAGTAAGCACAGGCA
Mouse	<i>Il10</i>	F: CCAAGCCTTATCGGAAATGA
		R: TCACTCTTCACCTGCTCCAC
Mouse	<i>Tgfb</i>	F: TCCTTGCCCTGCGGAAGTG
		R: GGAGAGCATTGAGCAGTTCGA
Mouse	<i>Tnfsf14</i>	F: CTGCATCAACGTCTTGGAGA
		R: GATACGTCAAGCCCCTCAAG
Mouse	<i>Egfr<sup>A</sup></i>	F: CCTCGTCTGTGGAAGAACTA
		R: CTCAGCCAGATGATGTTGAC
Mouse	<i>Tbx21</i>	F: GCCAGGGAACCGCTTATATG
		R: GACGATCATCTGGGTACATTGT
Mouse	<i>Ifng</i>	F: GGCCATCAGCAACAACATAAGCGT
		R: TGGGTTGTTGACCTCAAACCTTGGC
Mouse	<i>Rorc</i>	F: CCGCTGAGAGGGGCTTCAC
		R: TGCAGGAGTAGGCCACATTACA
Mouse	<i>Il17a</i>	F: ATCCCTCAAAGCTCAGCGTGTC
		R: GGGTCTTCATTGCGGTGGAGAG
Mouse	<i>Foxp3</i>	F: GAGAGCAGGCAGTTCAGGAC
		R: CGGGAGCATATACCAGGCAC
Mouse	<i>Il23a</i>	F: CCAGCAGCTCTCTCGGAATC
		R: TCATAGTCCCGCTGGTGC
Mouse	<i>Lysm</i>	F: TGGGATCAATTGCAGTGCT
		R: CACCACCCTCTTTGCACATT
Mouse	<i>Cre</i>	F: GATTTGACCCAGGTTTCGTTT
		R: GCTAACCCAGCGTTTTTCGTTT

**Supplemental Table 2. List of primers used for PCR and RT-PCR.** <sup>A</sup>Indicates primers were used to confirm excision of the *Egfr* alleles in *Egfr<sup>Δmye</sup>* mice.

<b>Antibody</b>	<b>Dilution</b>	<b>Application</b>	<b>Source (Location)</b>
Rabbit polyclonal anti-pEGFR Y1068	1:1,000	WB	Cell Signaling (Danvers, MA) Cat. No. 2234
Rabbit polyclonal anti-pEGFR S1046/47	1:1,000	WB	Cell Signaling (Danvers, MA) Cat. No. 2238
Rabbit polyclonal anti-tEGFR	1:5,000 1:100 1:50	WB IF FC	Cell Signaling (Danvers, MA) Cat. No. 2232
Mouse monoclonal anti-β-actin	1:10,000	WB	Sigma-Aldrich (St. Louis, MO) Cat. No. A1978
Rabbit polyclonal anti-MyD88	1:1000	WB	Cell Signaling (Danvers, MA) Cat. No. 3699
Rabbit polyclonal anti-pIKBK S176/180	1:2000	WB	Cell Signaling (Danvers, MA) Cat. No. 2697
Rabbit polyclonal anti-tIKBK	1:2000	WB	Cell Signaling (Danvers, MA) Cat. No. 2682
Mouse monoclonal anti-pNFKBIA S32/36	1:1000	WB	Life Technologies (Carlsbad, CA) Cat. No. MA515224
Rabbit polyclonal anti-tRELA	1:5,000	WB	EMD Millipore (Billerica, MA) Cat. No. PC138
Rabbit polyclonal anti-FBL	1:5,000	WB	Santa Cruz (Dallas, TX) Cat. No. SC-25397
Mouse monoclonal anti-GAPDH	1:10,000	WB	EMD Millipore (Billerica, MA) Cat. No. MAB374
Goat anti-mouse IgG, HRP labeled	1: 30,000	WB	Jackson ImmunoResearch (St. Louis, MO) Cat. No. 115-035-003
Goat anti-rabbit IgG, HRP labeled	1:3,000- 1:6,000	WB	Jackson ImmunoResearch (St. Louis, MO) Cat. No. 111-035-003
Rabbit polyclonal anti-NOS2	1:5,000 1:100	WB FC	Pierce (Waltham, MA)**
Rabbit polyclonal anti-Cldv CASP3 D175	1:400	IF	Cell Signaling (Danvers, MA) Cat. No. 9661
Anti-mouse F4/80-Alexa488	1:100	FC	Invitrogen (Carlsbad, CA) Cat. No.
Anti-mouse F4/80-PE	1:100	FC	Invitrogen (Carlsbad, CA) Cat. No. MF48004
Anti-mouse CD4-PerCP-Cy5.5	1:200	FC	Biolegend (San Diego, CA) Cat. No. 100540
Hamster anti-mouse IFNG-FITC	1:100	FC	BD Biosciences (San Jose, CA) Cat. No. 562019
Rat anti-mouse IL-17A-PE	1:100	FC	BD Biosciences (San Jose, CA) Cat. No. 561020
Anti-mouse CD25-PE	1:100	FC	eBioscience (San Diego, CA) Cat. No. 12-0281-83
Rat anti-mouse FOXP3-Alexa488	1:00	FC	BD Biosciences (San Jose, CA) Cat. No. 560407
Mouse monoclonal Pan-cytokeratin PE	1:100	FC	Abcam (Cambridge, UK) Cat. No. AB52460
Rat anti-mouse CD11b-FITC	1:100	FC	Biolegend (San Diego, CA) Cat. No. 101219
Rant anti-mouse CD11b-PE-Cy7	1:100	FC	BD Biosciences (San Jose, CA) Cat. No. 552850

Hamster anti-mouse CD11c-PE-Cy7	1:100	FC	BD Biosciences (San Jose, CA) Cat. No. 558079
Anti-mouse H2-AB1-PerCP-Cy5.5	1:100	FC	Biolegend (San Diego, CA) Cat. No. 562363
Goat Anti-rabbit IgG-Alexa488	1:200	FC	Jackson ImmunoResearch (St. Louis, MO) Cat. No. 111-095-003
Rabbit IgG (isotype control)	1:50	FC	Jackson ImmunoResearch (St. Louis, MO) Cat. No. 011-000-003
Rabbit polyclonal anti-pEGFR	Pre-diluted	IF/IHC	Biocare Medical (Concord, CA) Cat. No. API 300
Rabbit HRP Polymer	Pre-diluted	IF/IHC	Biocare Medical (Concord, CA) Cat. No. RHRP520
Goat anti-HRP, Alexa488	1:400	IF	Jackson ImmunoResearch (St. Louis, MO) Cat. No. 123-545-021
Mouse monoclonal anti-CD68	Pre-diluted	IF	Santa Cruz Biotechnology (West Grove, PA) Cat. No. SC-7084
Goat anti-mouse IgG, Alexa555	1:500	IF	Life Technologies (Carlsbad, CA) Cat. No. A31570
Rat polyclonal anti-F4/80	1:50	IF	Invitrogen (Carlsbad, CA) Cat. No. MF48000
Rabbit anti-rat IgG, TRITC	1:100	IF	Sigma-Aldrich (St. Louis, MO) Cat. No. T4280
Mouse Anti-TNF- $\alpha$	10 ng/mL	NEUT	Cell Signaling (Danvers, MA) Cat. No. 11969
Mouse Anti-HB-EGF	25 ng/mL	NEUT	Sigma-Aldrich (St. Louis, MO) Cat. No. AF259NA

**Supplemental Table 3. A list of all antibodies used for this study, including the dilution, application and company from which the antibodies were purchased. WB = western blotting, FC = flow cytometry, IF = immunofluorescence, IHC = immunohistochemistry. NEUT = neutralization. \*\*No longer available.**

## Supplemental References

1. Van Kaer, L., Algood, H.M., Singh, K., Parekh, V.V., Greer, M.J., Piazuelo, M.B., Weitkamp, J.H., Matta, P., Chaturvedi, R., Wilson, K.T., et al. 2014. CD8 $\alpha\alpha$ (+) innate-type lymphocytes in the intestinal epithelium mediate mucosal immunity. *Immunity* 41:451-464.
2. Gobert, A.P., Cheng, Y., Akhtar, M., Mersey, B.D., Blumberg, D.R., Cross, R.K., Chaturvedi, R., Drachenberg, C.B., Boucher, J.L., Hacker, A., et al. 2004. Protective role of arginase in a mouse model of colitis. *J. Immunol.* 173:2109-2117.
3. Singh, K., Chaturvedi, R., Barry, D.P., Coburn, L.A., Asim, M., Lewis, N.D., Piazuelo, M.B., Washington, M.K., Vitek, M.P., and Wilson, K.T. 2011. The apolipoprotein E-mimetic peptide COG112 inhibits NF- $\kappa$ B signaling, proinflammatory cytokine expression, and disease activity in murine models of colitis. *J. Biol. Chem.* 286:3839-3850.
4. Gobert, A.P., Verriere, T., Asim, M., Barry, D.P., Piazuelo, M.B., de Sablet, T., Delgado, A.G., Bravo, L.E., Correa, P., Peek, R.M., Jr., et al. 2014. Heme oxygenase-1 dysregulates macrophage polarization and the immune response to *Helicobacter pylori*. *J. Immunol.* 193:3013-3022.
5. Chaturvedi, R., Asim, M., Piazuelo, M.B., Yan, F., Barry, D.P., Sierra, J.C., Delgado, A.G., Hill, S., Casero Jr, R.A., Bravo, L.E., et al. 2014. Activation of EGFR and ErbB2 by *Helicobacter pylori* results in survival of gastric epithelial cells with DNA damage. *Gastroenterology* 146:1739-1751.
6. Lewis, N.D., Asim, M., Barry, D.P., de Sablet, T., Singh, K., Piazuelo, M.B., Gobert, A.P., Chaturvedi, R., and Wilson, K.T. 2011. Immune evasion by *Helicobacter pylori* is mediated by induction of macrophage arginase II. *J. Immunol.* 186:3632-3641.
7. Everhart, M.B., Han, W., Sherrill, T.P., Arutiunov, M., Polosukhin, V.V., Burke, J.R., Sadikot, R.T., Christman, J.W., Yull, F.E., and Blackwell, T.S. 2006. Duration and intensity of NF- $\kappa$ B activity determine the severity of endotoxin-induced acute lung injury. *J. Immunol.* 176:4995-5005.
8. Han, W., Li, H., Cai, J., Gleaves, L.A., Polosukhin, V.V., Segal, B.H., Yull, F.E., and Blackwell, T.S. 2013. NADPH oxidase limits lipopolysaccharide-induced lung inflammation and injury in mice through reduction-oxidation regulation of NF- $\kappa$ B activity. *J. Immunol.* 190:4786-4794.
9. Coburn, L.A., Gong, X., Singh, K., Asim, M., Scull, B.P., Allaman, M.M., Williams, C.S., Rosen, M.J., Washington, M.K., Barry, D.P., et al. 2012. L-arginine supplementation improves responses to injury and inflammation in dextran sulfate sodium colitis. *PLoS One* 7:e33546.